

# Action Minimization and Sharp-Interface Limits for the Stochastic Allen-Cahn Equation

(Preliminary version. Please do not distribute.)

Robert V. Kohn,<sup>\*</sup>Felix Otto,<sup>†</sup>Maria G. Reznikoff,<sup>‡</sup>  
and Eric Vanden-Eijnden<sup>§</sup>

March 25, 2005

## Abstract

We study the action minimization problem which is formally associated to phase transformation in the stochastically perturbed Allen-Cahn equation. The sharp-interface limit is related to (but different from) the sharp-interface limits of the related energy functional and deterministic gradient flows. In the sharp-interface limit of the action minimization problem, we find distinct “most likely switching pathways,” depending on the relative costs of nucleation and propagation of interfaces. This competition is captured by the limit of the action functional, which we derive formally and propose as the natural candidate for the  $\Gamma$ -limit. Guided by the reduced functional, we prove upper and lower bounds for the minimal action which agree on the level of scaling.

---

<sup>\*</sup>Courant Institute of Mathematical Sciences, New York University, USA, kohn@cims.nyu.edu.

<sup>†</sup>Institut für Angewandte Mathematik, Universität Bonn, Germany, otto@iam.uni-bonn.de.

<sup>‡</sup>Institut für Angewandte Mathematik, Universität Bonn, Germany, reznikoff@iam.uni-bonn.de.

<sup>§</sup>Courant Institute of Mathematical Sciences, New York University, USA, eve2@cims.nyu.edu.

# Contents

<b>1</b>	<b>Introduction</b>	<b>3</b>
<b>2</b>	<b>The reduced action functional</b>	<b>11</b>
<b>3</b>	<b>Upper bounds: constructions</b>	<b>14</b>
3.1	Dimension $d = 1$ . . . . .	14
3.2	Higher space dimensions . . . . .	20
3.2.1	One-dimensional constructions . . . . .	22
3.2.2	Connection with curvature flow . . . . .	22
3.2.3	MCF-based constructions . . . . .	23
3.2.4	Accelerated curvature flow . . . . .	25
<b>4</b>	<b>Lower bounds</b>	<b>26</b>
4.1	Scaling bound . . . . .	27
4.2	Sharp 1-d bound, under two assumptions . . . . .	28
4.3	Ansatz-free bounds and equipartition of energy . . . . .	30
<b>5</b>	<b>Outlook</b>	<b>36</b>
<b>A</b>	<b>Two other action regimes</b>	<b>37</b>
A.1	Short-time limit . . . . .	38
A.2	Energy-barrier regime . . . . .	39
A.2.1	Energy barrier regime: small systems . . . . .	40
A.2.2	Energy barrier regime: large systems . . . . .	41
<b>B</b>	<b>The energy and its saddle points</b>	<b>43</b>
B.1	Small systems . . . . .	43
B.2	The birth of a new saddle point . . . . .	45
B.3	Bigger systems in higher dimensions . . . . .	46

Keywords: *Allen-Cahn equation, stochastic partial differential equations, large deviation theory, action minimization, sharp-interface limits*

# 1 Introduction

At the mean field level, phase transformation can be studied within the framework of Ginzburg-Landau theory. It describes the state of the system in terms of a scalar order parameter,  $u$ , defined in a domain  $\Omega \subset \mathbb{R}^d$ , and a free energy:

$$E^\varepsilon[u] = \int_{\Omega} \left( \frac{|\nabla u|^2}{2} + \varepsilon^{-2}V(u) \right) dx. \quad (1.1)$$

The gradient term penalizes spatial variation, and the potential  $V$  has a double-well shape with minima at the preferred states of the order parameter; the relative strength of the two terms is measured by the parameter  $\varepsilon$ . A canonical example of  $V$  is given by

$$V(u) = \frac{1}{4}(1 - u^2)^2, \quad (1.2)$$

and for simplicity, we restrict our attention to this potential. Generalization to other choices of equal-well potentials for  $V$  is possible. (This changes the value of the constant  $c_0$ , which appears, for example, in Definitions 1 and 2 below.)

The  $L^2$ -gradient flow for (1.1) is the Allen-Cahn equation:

$$\dot{u} = \Delta u - \varepsilon^{-2}V'(u). \quad (1.3)$$

(Throughout,  $\dot{u}$  denotes the time derivative of  $u$ .) The only two stable fixed points of the dynamics (1.3) are the pure states  $u_- \equiv -1$  and  $u_+ \equiv +1$  (for periodic or Neumann boundary conditions). An energy barrier separates them, and initial conditions close to  $u_-$  never visit  $u_+$ .

As soon as thermal effects are taken into account, the picture changes. Even for small thermal noise, an initial state  $u(\cdot, 0) = u_-$  will eventually undergo phase transformation (or “switching”), driven over the energy barrier and into a small neighborhood of  $u_+$ . A natural way to include a noise term in (1.3) is via the stochastically perturbed Allen-Cahn equation:

$$\dot{u} = \Delta u - \varepsilon^{-2}V'(u) + \sqrt{2\gamma} \eta_\lambda. \quad (1.4)$$

Here  $\gamma$  is a parameter measuring the temperature of the system, and  $\eta_\lambda$  is a spatially regularized noise:

$$\eta_\lambda := \phi_\lambda * \eta,$$

where  $*$  denotes convolution,  $\phi_\lambda(x) = \lambda^{-d}\phi(x/\lambda)$  for  $\phi$  an approximate identity, and  $\eta$  is a standard space-time white noise, i.e. a Gaussian process with

mean zero and covariance  $\mathbb{E}(\eta(x, t)\eta(x', t')) = \delta(x - x')\delta(t - t')$ . The parameter  $\lambda$  measures the correlation length in the noise, and  $\lambda = 0$  leads formally to an invariant measure which is the Gibbs distribution for the energy (1.1) with temperature  $\gamma$ .

The main objective of the paper is to study phase transformation in the sharp-interface limit,  $\varepsilon \rightarrow 0$ . The noise term in (1.4) introduces two additional parameters,  $\gamma$  and  $\lambda$ . We are interested in the limit in which all three parameters go to zero. The limit  $\gamma \rightarrow 0$  is interesting because it is the small temperature regime in which the stochastic dynamics in (1.4) are not dominated by the noise term, but rather involve an interplay between the deterministic and stochastic parts. As mentioned above, the limit  $\lambda \rightarrow 0$  is distinguished by being (formally) consistent with the Gibbs distribution. Finally, the sharp-interface limit,  $\varepsilon \rightarrow 0$ , leads to a reduced problem in which the switching pathway is characterized by the generation and propagation of interfaces (see below). In this paper, we study a specific order of the limits; namely, we take  $\gamma \rightarrow 0$  first, then  $\lambda \rightarrow 0$ , and finally  $\varepsilon \rightarrow 0$ . This limit is analytically accessible because it allows us to study the problem using large deviation theory, and even though (1.4) is ill-posed for  $\lambda = 0$  in dimension  $d > 1$ , it is possible to study  $\lambda \rightarrow 0$  after first letting  $\gamma \rightarrow 0$ , as we explain in the following discussion. A more general analysis of the behavior of (1.4) in terms of  $(\varepsilon, \gamma, \lambda)$  is an interesting but complicated topic. We comment briefly on the question of permuting the limits in Section 5.

**Large deviations.** The probability of a stochastically driven barrier-crossing event is estimated by the Wentzell-Freidlin theory of large deviations in terms of an *action functional*. If we define the set

$$\mathcal{A} := \{u(\cdot, 0) = u_-, u(\cdot, t) \in \text{nbid}(u_+) \text{ for some } t \leq T\},$$

then for  $\gamma \ll 1$ , the probability of switching under the dynamics (1.4) in time  $T$  is roughly estimated by

$$\text{Prob}(\mathcal{A}) \approx \exp\left(-\inf_{u \in \mathcal{A}} S^{\varepsilon, \lambda}[u]/\gamma\right), \quad (1.5)$$

where the action functional is

$$S^{\varepsilon, \lambda}[u] = \frac{1}{4} \int_0^T \int_{\Omega} \int_{\Omega} (\mathcal{F}u(x, t), K_{\lambda}^{-1}(x, y)\mathcal{F}u(y, t)) dy dx dt, \quad (1.6)$$

for all  $u$  such that this quantity is defined, and infinity otherwise. Here, we have defined

$$\mathcal{F}u(x, t) := \dot{u}(x, t) - \Delta u(x, t) + \varepsilon^{-2}V'(u(x, t)),$$

and  $K$  is the spatial covariance operator of  $\eta_\lambda$ , i.e.

$$\mathbb{E}(\eta_\lambda(x, t)\eta_\lambda(y, t)) = K_\lambda(x - y)\delta(t - s).$$

Furthermore, the minimizer of the action functional over  $\mathcal{A}$  is the *most likely switching pathway*, the deterministic trajectory which is approximated by the noisy path as it crosses the energy barrier (with probability one, in the limit as  $\gamma \rightarrow 0$ ). For a complete discussion, see [14, 39, 6].

Taking the limit in (1.6) as the correlation length vanishes leads to:

$$S^\varepsilon[u] = \frac{1}{4} \int_0^T \int_\Omega (\dot{u} - \Delta u + \varepsilon^{-2}V'(u))^2 dx dt. \quad (1.7)$$

In dimension  $d = 1$ , where the stochastic equation is well-defined even with a space-time white noise, Faris and Jona-Lasinio [12] prove that (1.7) is the action functional for (1.4) on the space of continuous functions. Although the stochastic pde with  $\lambda = 0$  is ill-posed in higher dimensions, the behavior of (1.7) controls the behavior of observables (such as the mean switching time between  $u_-$  and  $u_+$ ) for  $\lambda \ll 1$ , at least in an appropriate regime of the  $(\varepsilon, \gamma, \lambda)$  parameter space.

Motivated by these ideas, we study the action minimization problem

$$\inf_{\substack{u(\cdot, 0) = u_- \\ u(\cdot, T) = u_+}} S^\varepsilon[u].$$

For simplicity, we focus on  $\Omega = [0, L]^d$  and periodic boundary conditions. The cases of Neumann and homogeneous-Dirichlet boundary conditions are conceptually the same, requiring only minor modification of the assertions; we comment occasionally on similarities and differences.

**Sharp-interface limit: deterministic.** When  $\varepsilon \ll 1$  in (1.1) or (1.3), the field  $u$  is forced to concentrate on  $\pm 1$  except possibly at sharp interfaces between the two phases. The sharp-interface limit  $\varepsilon \rightarrow 0$  corresponds to the limit of infinite scale separation between the interfacial length scale and the system size, and has been studied previously both on the level of the energy functional and the deterministic dynamics.

Any sequence  $u_\varepsilon$  with uniformly bounded renormalized energy,

$$\hat{E}^\varepsilon[u] := \varepsilon E^\varepsilon[u] = \int_\Omega \left( \frac{\varepsilon |\nabla u|^2}{2} + \varepsilon^{-1}V(u) \right) dx, \quad (1.8)$$

converges as  $\varepsilon \rightarrow 0$  (up to a subsequence) to a function which is a.e.  $\pm 1$ , with an interface  $\partial\{u = 1\}$  of finite perimeter. Moreover, Modica and Mortola

[26, 27] proved the  $\Gamma$ -convergence of the renormalized energy to the perimeter functional:

$$\hat{E}^\varepsilon[\cdot] \xrightarrow{\Gamma} c_0 P[\cdot],$$

where here and throughout, the constant  $c_0$  corresponding to the potential  $V$  defined in (1.2) is  $c_0 := 2\sqrt{2}/3$ . (In brief,  $\Gamma$ -convergence is a notion of convergence for variational problems which implies, in particular, that minimizers converge to minimizers of the limit problem, and which is stable under compact perturbations. See, for instance, [1].)

Given the  $\Gamma$ -convergence of the energy, one would like to know what becomes of the deterministic gradient flow in the sharp-interface limit. Is the limit of the gradient flow equal to the gradient flow for the limiting energy? It is known [36, 8, 11, 20] that in dimension  $d > 1$ , (1.3) leads to limiting dynamics in which the interface  $\partial\{u = 1\}$  evolves by mean-curvature-flow (MCF), i.e.

$$v_n = -\kappa, \tag{1.9}$$

where  $v_n$  is the normal velocity of the interface and  $\kappa$  is the mean curvature. Because curvature flow is the gradient flow of perimeter with respect to  $L^2$  of the interface, we see that in this sense, the limiting dynamics are indeed the gradient flow of the limiting energy. (The change of metric – from  $L^2$  in the bulk to  $L^2$  on the interface – is related to the slowing down of the dynamics as  $\varepsilon \rightarrow 0$ .) In one space dimension, the situation is somewhat degenerate; here, the interfaces are points and the slow motion of the interfaces has no effect on the leading order term in the energy. Driven instead by the exponentially small correction terms in the energy, the interface motion is exponentially slow [4, 16, 3].

**Sharp-interface limit: action functional.** The central question in this paper is what happens to the renormalized action functional,

$$\hat{S}^\varepsilon[u] := \varepsilon S^\varepsilon[u] = \frac{1}{4} \int_0^T \int_\Omega (\varepsilon^{1/2} \dot{u} + \varepsilon^{-1/2} (-\varepsilon \Delta u + \varepsilon^{-1} V'(u)))^2 dx dt, \tag{1.10}$$

in the sharp-interface limit. We show that the minimum action

$$\hat{S}_{switch} := \inf_{\substack{u(\cdot, 0) = u_- \\ u(\cdot, T) = u_+}} \hat{S}^\varepsilon[u] \tag{1.11}$$

remains bounded and nontrivial as  $\varepsilon \rightarrow 0$  by developing  $\varepsilon$ -independent upper and lower bounds. In other words,  $\hat{S}^\varepsilon[\cdot]$  indeed represents the correctly renormalized action functional. Moreover, our upper bound constructions suggest

the following candidates for the  $\Gamma$ -limit of (1.10). In dimension  $d > 1$ , the candidate for the  $\Gamma$ -limit is

$$S_{nuc} + \frac{c_0}{4} \int_0^T \int_{\Gamma(t)} (v_n + \kappa)^2 d\sigma dt, \quad (1.12)$$

where  $S_{nuc}$  is the nucleation cost,  $\Gamma(t)$  is the interface at time  $t$ ,  $v_n$  is the normal velocity, and  $\kappa$  is curvature. (The nucleation cost is the jump in action which results from the energy jump if  $(d - 1)$ -dimensional interfaces are generated.) We use our upper bound constructions in Subsection 3.2 to prove that in  $d = 2$ , for instance, action minimizing pathways *must* have higher dimensional spatial structure (i.e. they cannot be merely one-dimensional).

The degeneracy in dimension  $d = 1$  makes the situation slightly different. There is no notion of curvature, and the contribution of the energy vanishes in the limit. The candidate for the  $\Gamma$ -limit in  $d = 1$  is

$$S_{nuc} + \frac{c_0}{4} \sum_{i=1}^N \int_0^T \dot{g}_i(t)^2 dt, \quad (1.13)$$

where  $g_i(t)$  is the position of the  $i^{th}$  interface at time  $t$ . Whereas in higher dimensions there is no nucleation cost for lower dimensional interfaces (interfaces of dimension less than  $d - 1$ ), in dimension  $d = 1$  there is no possibility to avoid a nucleation cost.

An elementary argument produces a lower bound which matches our upper bounds in terms of *scaling* (cf. Section 4). Proving sharp, ansatz-free lower bounds for (1.10) – which is necessary in order to justify the  $\Gamma$ -limit candidates suggested above – goes beyond the scope of this paper. We explain in Section 4, however, how the limiting behavior of the associated energy measures and equipartition between the bulk and gradient terms in the energy, (1.8), are linked to proving a lower bound for the action functional. These ideas are used in [21] to prove rigorous results for the case  $d = 1$ . In some sense, it is not surprising that equipartition of energy plays a role in the action problem, since it is important in proving convergence of the Allen-Cahn dynamics to Brakke’s notion of curvature flow [20].

Is the sharp-interface limit of the action functional the action functional of sharp-interface gradient flow? Formally, we give a positive answer by identifying the limiting action, (1.12). Indeed, given a gradient flow, one can view the  $\Gamma$ -convergence of the associated energy functional and the (nondegenerate)  $\Gamma$ -convergence of the decoupled action functional (1.17) as sufficient conditions for the convergence of the dynamics to the gradient flow for the limiting energy, much in the spirit of Sandier and Serfaty [37].

On the deeper level of the stochastic problem, one would like to know whether this limiting action is in fact the action functional for a well-defined stochastic process and, moreover, whether this process is the sharp-interface limit of the process defined by (1.4). See Section 5 for additional comments.

**Initial observations and heuristics.** We conclude the introduction by explaining some basic properties of the action functional, and the heuristic picture for  $d = 1$ . In particular, we explain the connection between the energy and action functionals, and how a competition between the costs of forming and transporting interfaces emerges in the sharp-interface limit.

The most fundamental relationship between the action and energy functionals is revealed by the fact that for any  $t \in (0, T]$ :

$$\begin{aligned} \hat{S}^\varepsilon[u] &\geq \frac{1}{4} \int_0^t \int_\Omega \left( \varepsilon^{1/2} \dot{u} + \varepsilon^{-1/2} D_u \hat{E}^\varepsilon(u) \right)^2 dx dt' \\ &= \frac{1}{4} \int_0^t \int_\Omega \left( \left( \varepsilon^{1/2} \dot{u} - \varepsilon^{-1/2} D_u \hat{E}^\varepsilon(u) \right)^2 + 4 \dot{u} D_u \hat{E}^\varepsilon(u) \right) dx dt' \\ &\geq \hat{E}^\varepsilon[u(\cdot, t)] - \hat{E}^\varepsilon[u(\cdot, 0)]. \end{aligned} \tag{1.14}$$

(We have used  $D_u \hat{E}^\varepsilon := -\varepsilon \Delta u + \varepsilon^{-1} V'(u)$  as shorthand for the functional derivative of the energy in  $L^2$ , and in the third line we have used the boundary conditions to integrate by parts.) An immediate consequence is that the minimal action is bounded below by the energy barrier between  $u_-$  and  $u_s$ , the minimum-energy saddle point (which we will also call the minimal saddle):

$$\hat{S}_{switch} \geq \hat{E}^\varepsilon[u_s] - \hat{E}^\varepsilon[u_-] =: \Delta \hat{E}^\varepsilon. \tag{1.15}$$

(For periodic or Neumann boundary conditions, the barrier is exactly equal to the energy of  $u_s$ ; for zero-Dirichlet boundary conditions, there is a correction due to the nonzero energy of  $u_-$ .) Looked at from a slightly different point of view, (1.14) shows that functions with bounded action are bounded in energy at every time,  $t \leq T$ . Thus, while action minimizers are not energy minimizers, their energy is uniformly bounded in time.

The calculation in (1.14) also characterizes the long-time action minimizing trajectory in terms of the deterministic Allen-Cahn dynamics. An action which is strictly *equal* to the energy barrier can only be achieved by a path which flows through the minimal saddle and satisfies

$$\dot{u} = \begin{cases} +\varepsilon^{-1} D_u \hat{E}^\varepsilon(u) & t \leq t' \\ -\varepsilon^{-1} D_u \hat{E}^\varepsilon(u) & t' < t \leq T, \end{cases} \tag{1.16}$$



with

$$u(\cdot, 0) \equiv -1, \quad u(\cdot, t') = u_s, \quad u(\cdot, T) \equiv +1.$$

(We remark that the first part of (1.16) is well-posed only as a boundary value problem connecting  $u_-$  and  $u_s$ .) Such an “ideal” pathway requires infinite time, but for switching times which are large compared to the deterministic timescale, an approximation of the pathway (modified near the critical points) achieves a nearly optimal action, cf. Appendix A.

When the switching time  $T$  is short compared to the deterministic timescale, on the other hand, the action minimization problem is more complicated. The sharp-interface limit is a regime in which the full action minimization problem reduces to a competition between two costs: the cost to form interfaces and the cost to move them. We call the former the nucleation cost and the latter the propagation cost. (We use the term “nucleation” in a loose sense here; see Remark 1, below.) The action minimizing trajectory strikes an optimal balance between these costs, depending on the relative size of the switching time,  $T$ , and the system size,  $L$ . The phenomenon of competing nucleation and propagation costs was studied in [9] and also (for  $d = 1$ ) in [13]; the same phenomenon is also investigated for a different but related one-dimensional model in [7].

To capture the main idea of the competition between nucleation and propagation costs in the action, consider the case  $d = 1$ . Each point nucleation incurs a cost. On the other hand, moving the interfaces across the system within time  $T$  also incurs a cost, and the more interfaces there are, the less distance that each must travel. (See Figure 3.) The back-of-the-envelope calculation which compares these two costs is the following. Assume a fixed cost per nucleation and a periodic structure, so that there are  $L/\ell$  nucleations, spaced  $\ell$  apart. The nucleation cost is  $\sim L/\ell$ . Estimating the propagation cost by the transportation term in the action yields a cost  $\sim L\ell/T$ . Balancing these costs implies  $\ell = \sqrt{T}$ , and a minimal action which scales like  $L/\sqrt{T}$ .

Finally, the boundary conditions and the initial and final conditions also imply that the action decouples as:

$$\begin{aligned} & \frac{1}{4} \int_0^T \int_{\Omega} \left( \varepsilon^{1/2} \dot{u} + \varepsilon^{-1/2} D_u \hat{E}^\varepsilon(u) \right)^2 dx dt \\ &= \frac{1}{4} \int_0^T \int_{\Omega} \left( \varepsilon \dot{u}^2 + \varepsilon^{-1} (D_u \hat{E}^\varepsilon(u))^2 \right) dx dt. \end{aligned} \quad (1.17)$$

The penalization of the second term suggests using hyperbolic tangent profiles or, more precisely, using constructions in which  $u_\varepsilon(x, t)$  is defined in terms of the hyperbolic tangent of the distance from  $x$  to the interface,  $\Gamma(t)$ , cf. Section 2.

**Two other scaling regimes.** Given the action functional:

$$S^{L,T}[u] := \int_0^T \int_{\Omega_L} (\dot{u} - \Delta u + V'(u))^2 dx dt, \quad (1.18)$$

one passes to the sharp-interface regime by considering  $L \rightarrow \infty$ ,  $T \rightarrow \infty$ , with the diffusive scaling,  $L \sim \sqrt{T} =: \varepsilon^{-1}$ . This is the most interesting scaling, because of the competition between nucleation cost and propagation cost. More generally, however, the minimization problem:

$$S_{switch} := \inf_{\substack{u(\cdot,0)=u_- \\ u(\cdot,T)=u_+}} S^{L,T}[u],$$

is an implicit function of the two parameters,  $L$  and  $T$ , and other limits may of course also be considered. We point out two additional scaling regimes of the action, the short-time limit ( $T \rightarrow 0$  with  $L$  fixed) and the energy-barrier regime ( $L, T \rightarrow \infty$  with  $L \ll \sqrt{T}$ ). These regimes are easy to understand; see Appendix A.

In the energy-barrier regime, the action depends on the minimum-energy saddle point, which in turn depends on the system size. We study this dependence in Appendix B. In particular, we look at the crossover from  $u \equiv 0$  to a spatially nonuniform saddle as the energy minimizing saddle point, and at the limiting energy of this minimal saddle as the domain becomes large (or, equivalently, as  $\varepsilon$  vanishes).

**Organization.** In Section 2, we present the reduced action functional and a heuristic derivation. We prove the scaling of the action in the sharp-interface regime by developing matching upper and lower bounds. In Section 3, we introduce the upper bound constructions. For  $d > 1$ , we introduce one-dimensional, mean-curvature-flow, and accelerated mean-curvature-flow constructions. In Section 4, we turn to the question of lower bounds. We prove a lower bound for the scaling, and investigate what would be necessary in order to improve the result to a sharp bound. In Section 5 we conclude with some additional connections and open problems. In Appendix A, we consider two (simple) limits other than the sharp-interface limit, namely the short-time limit and the energy-barrier regime. Finally, in Appendix B, we study the dependence of the energy on the system size.

**Remark 1.** *We use the term “nucleation” to mean the nucleation of a new phase. Classically, the term nucleation event is often used to mean passing through a saddle point. In the case where  $V$  is an asymmetric double-well potential, for instance, the minimum-energy saddle point is a droplet which*

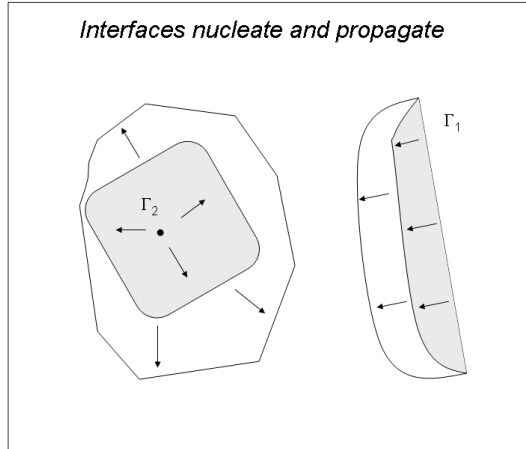


Figure 1: Interfaces forming and propagating in a two-dimensional system. The reduced action functional counts the perimeter of nucleated structures and the propagation cost of moving against curvature.

*is localized, and nucleation refers to passing through this well-defined point in phase space. In the setting of the symmetric double-well, there is no localized droplet, or, in other words, the minimum-energy saddle point does not converge as the system size goes to infinity. For us, nucleation means the generation of an interface connecting  $u \approx -1$  with  $u \approx +1$ .*

## 2 The reduced action functional

In this section, we present the candidate for the  $\Gamma$ -limit of the renormalized action functional, (1.10). One can view our argument either as a formal derivation or as a building block for the upper-bound half of a  $\Gamma$ -limit argument. (We use the structure of the reduced action functional to develop upper bound constructions in Section 3.) A matching lower bound requires an analysis of the limiting energy measures; see Section 4 and also [21], for  $d = 1$ .

We begin by defining:

**Definition 1.** *The reduced action functional for the family of interfaces  $\Gamma(t)$ ,  $t \in [0, T]$ , is*

$$S^R[\Gamma(\cdot)] := S_1^R[\Gamma(\cdot)] + S_2^R[\Gamma(\cdot)], \quad (2.1)$$

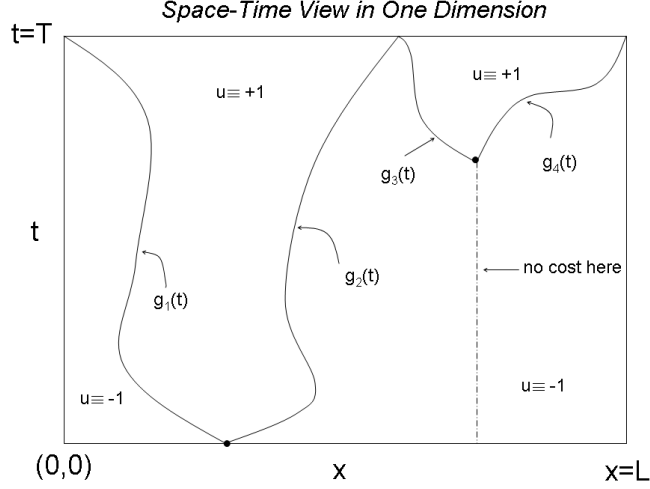


Figure 2: A space-time view of the sharp-interface limit of a switching path in one dimension. There are two nucleation events and the interfaces propagate in order to achieve switching by the rescaled switching time,  $t = T$ .

where

$$S_1^R[\Gamma(\cdot)] := \frac{c_0}{4} \int_0^T \int_{\Gamma(t)} (v_n + \kappa)^2 d\sigma dt, \quad S_2^R[\Gamma(\cdot)] := 2c_0 \sum_i \mathcal{H}^{d-1}(\Gamma_i).$$

Here,  $v_n$  and  $\kappa$  are the normal velocity and curvature of the interface. In  $d = 1$  we take the curvature of a point to be zero by definition.  $\mathcal{H}^{d-1}$  is the  $(d - 1)$ -dimensional Hausdorff measure and  $\Gamma_i$  is the  $i^{\text{th}}$  connected component of the interface at the time of creation of that component.

**Proposition 1.** For  $\varepsilon \downarrow 0$ , let  $u_\varepsilon(x, t)$  be a periodic, action minimizing sequence whose zero level sets converge to the smooth family of interfaces  $\Gamma(t)$ . Suppose that

$$u_\varepsilon(x, 0) \equiv -1, \quad u_\varepsilon(x, T) \equiv +1,$$

and that away from nucleation times,  $u_\varepsilon$  is of the form:

$$u_\varepsilon(x, t) = v(\varepsilon^{-1} d(x, \Gamma(t))), \quad (2.2)$$

(where  $d(\cdot)$  is the signed distance function). Then formally,

$$\lim_{\varepsilon \rightarrow 0} \hat{S}_\varepsilon[u_\varepsilon] = S^R[\Gamma(\cdot)].$$

It is worth distinguishing the higher dimensional case from the one-dimensional case. In  $d > 1$ , low dimensional nucleations are possible which incur no nucleation cost ( $S_2^R[\Gamma(\cdot)] = 0$ ). In contrast, for  $d = 1$ , nucleation cost is unavoidable. We emphasize the structure for  $d = 1$  in a separate corollary.

**Definition 2.** The reduced action functional in one dimension is given by

$$S^R[g(\cdot)] := \sum_{i=1}^{2M} \frac{c_0}{4} \int_0^T \dot{g}_i(t)^2 dt + 2M c_0. \quad (2.3)$$

Here, the interface is a finite collection of time-dependent points  $g(t) = \{g_i(t)\}_{i=1}^{2M}$ , where the  $g_i(t)$  give the location of the  $i^{\text{th}}$  interface at time  $t$ . (See Figure 2.)

**Corollary 1 (One dimension).** Suppose that  $u_\varepsilon(x, t)$  is a periodic, action minimizing sequence which satisfies the initial and final conditions and that away from nucleation times,

$$u_\varepsilon(x, t) = v(\varepsilon^{-1} d(x, g(t))).$$

Then formally,

$$\lim_{\varepsilon \rightarrow 0} \hat{S}_\varepsilon[u_\varepsilon] = S^R[g(\cdot)].$$

*Proof of Proposition 1.* We give a formal derivation of the reduced action functional. (An even simpler argument is possible for  $d = 1$ , using the ansatz from the corollary.) For the nucleation cost,  $S_2^R$ , we use a local estimate. Suppose that at time  $t_0$ , there is the nucleation of a  $(d - 1)$ -dimensional curve  $\Gamma_i$  of  $u \approx +1$  in a region of  $u \approx -1$ . The action cost for such an event is bounded below by the energy of the nucleated state, which converges to  $2c_0 \mathcal{H}^{d-1}(\Gamma_i)$  in the sharp-interface limit. Furthermore, this minimal cost can be achieved by reversing time along the heteroclinic orbit (as in the proof of Proposition 2 in Section 3, for instance).

To derive  $S_1^R$ , substitute (2.2) into the normalized functional  $\hat{S}^\varepsilon[u]$ . We deduce  $v(z) = \tanh(z/\sqrt{2})$  so that the highest order terms vanish. (We assume  $\Gamma(t)$  is a union of closed curves, and take the convention that distance is positive if and only if the point is interior to one of the curves. This is consistent with functions which nucleate regions of  $+1$ .) We use the properties of the distance function

$$|\nabla d| = 1, \quad \Delta d|_{\Gamma(t)} = -\kappa, \quad \frac{d}{dt} d(x, \Gamma(t)) = v_n,$$

to derive

$$\begin{aligned}
\hat{S}^\varepsilon[u] &\approx \frac{\varepsilon^{-1}}{8} \iint \operatorname{sech}^4\left(\frac{d(x, \Gamma(t))}{\varepsilon\sqrt{2}}\right) (v_n + \kappa)^2 dx dt \\
&= \frac{\varepsilon^{-1}}{8} \int_0^T \int_{s=-\infty}^{\infty} \int_{d=s} \operatorname{sech}^4\left(\frac{s}{\varepsilon\sqrt{2}}\right) (v_n + \kappa)^2 \mathcal{H}^0(d^{-1}(s) \cap \Omega) d\sigma ds dt \\
&= \frac{\varepsilon^{-1}}{8} \int_0^T \int_{s=-\infty}^{\infty} \operatorname{sech}^4\left(\frac{s}{\varepsilon\sqrt{2}}\right) \int_{d=s} (v_n + \kappa)^2 \mathcal{H}^0(d^{-1}(s) \cap \Omega) d\sigma ds dt,
\end{aligned}$$

where  $\sigma$  is the variable along the level curves of  $d$ , and the second to last equality follows by the coarea formula and the fact that  $|\nabla d| = 1$ . The multiplicity function  $\mathcal{H}^0$  restricts the integration to the spatial domain. Now, because the hyperbolic secant is sharply peaked, Laplace's method indicates that

$$\begin{aligned}
\hat{S}^\varepsilon[u] &\approx \frac{\varepsilon^{-1}}{8} \int_0^T \int_{\Gamma(t)} (v_n + \kappa)^2 d\sigma \int_{s=-\infty}^{\infty} \operatorname{sech}^4\left(\frac{s}{\varepsilon\sqrt{2}}\right) \mathcal{H}^0(d^{-1}(s) \cap \Omega) ds dt \\
&\xrightarrow{\varepsilon \rightarrow 0} \frac{c_0}{4} \int_0^T \int_{\Gamma(t)} (v_n + \kappa)^2 d\sigma dt.
\end{aligned}$$

□

We consider the implications of the reduced functionals below in Section 3.

## 3 Upper bounds: constructions

### 3.1 Dimension $d = 1$

The 1-d reduced action functional (2.3) reflects a cost for each nucleation point and a cost for propagation. The lowest cost is achieved by choosing equally spaced nucleation events and walls which propagate linearly in time. The constraint of switching means that the walls must cover the entire system by  $t = T$ , so that  $g_1(T) = 0$  and  $g_{2M}(T) = L$ . (See Figure 3 for an illustration.) The optimal number of walls minimizes

$$c_0 \left( 2N + \frac{L^2}{8NT} \right). \quad (3.1)$$

We use these ideas in the one-dimensional upper bound construction.

**Proposition 2 (Upper bound,  $d = 1$ ).** *For periodic boundary conditions and  $d = 1$ ,*

$$\limsup_{\varepsilon \rightarrow 0} \hat{S}_{switch} \leq \min_{N \in \mathbb{N}} \left( 2N + \frac{L^2}{8NT} \right) c_0.$$

The corresponding assertion for Neumann boundary conditions follows easily:

**Corollary 2.** *For Neumann boundary conditions and  $d = 1$ ,*

$$\limsup_{\varepsilon \rightarrow 0} \hat{S}_{switch} \leq \min_{N \in \mathbb{N}} \left( N + \frac{L^2}{4NT} \right) c_0.$$

*Proof.* We find it convenient to rescale space and time

$$\hat{x} := x/\varepsilon, \quad \hat{t} := t/\varepsilon^2,$$

and work with the  $\varepsilon$ -independent functional

$$S[u] := \int_0^{\hat{T}} \int_0^{\hat{L}} (\dot{u} - u_{\hat{x}\hat{x}} + V'(u))^2 d\hat{x} d\hat{t},$$

in the limit  $\hat{T} \rightarrow \infty, \hat{L} \rightarrow \infty, \hat{L}/\sqrt{\hat{T}} = c$ . For ease of notation, we drop the hats.

Let  $S_{[0,T]}$  denote the action on  $[0, T]$ . We need to show that for all  $\delta > 0$ , there exists a time  $T^*$  such that for all  $T \geq T^*$ ,

$$\inf_u S_{[0,T]}[u] \leq \min_{N \in \mathbb{N}} \left( 2N + \frac{L^2}{8NT} \right) c_0 + \delta.$$

We do this via explicit construction, demonstrating

$$\forall \delta > 0, \exists T^* \text{ such that}$$

$$\forall T \geq T^*, \exists u^{\delta, T} \text{ such that}$$

$$S_{[0,T]}[u^{\delta, T}] \leq \min_{N \in \mathbb{N}} \left( 2N + \frac{L^2}{8NT} \right) c_0 + \delta.$$

Our test function will consist of  $N$  periodic cells of length  $2\tilde{L} = L/N$ . At the center of each cell is a nucleation point. Consider the action on a single cell, where we center the construction at  $x = 0$  and take the system to be  $[-\tilde{L}, \tilde{L}]$ .

The construction proceeds in five stages. We first describe the stages and then explain how the parameters are chosen. We make use of the “nucleation state”

$$u_n(x) := \begin{cases} \tanh\left(\frac{L_1 + x}{\sqrt{2}}\right) & x \leq 0 \\ \tanh\left(\frac{L_1 - x}{\sqrt{2}}\right) & x > 0. \end{cases}$$

Note that  $u_n$  has a jump in the derivative at  $x = 0$ . For a first pass, we ignore this problem and present the main idea of the estimates. We then demonstrate that the discontinuity can be smoothed without loss. The same is true for the discontinuity that comes from “gluing” two cells together.

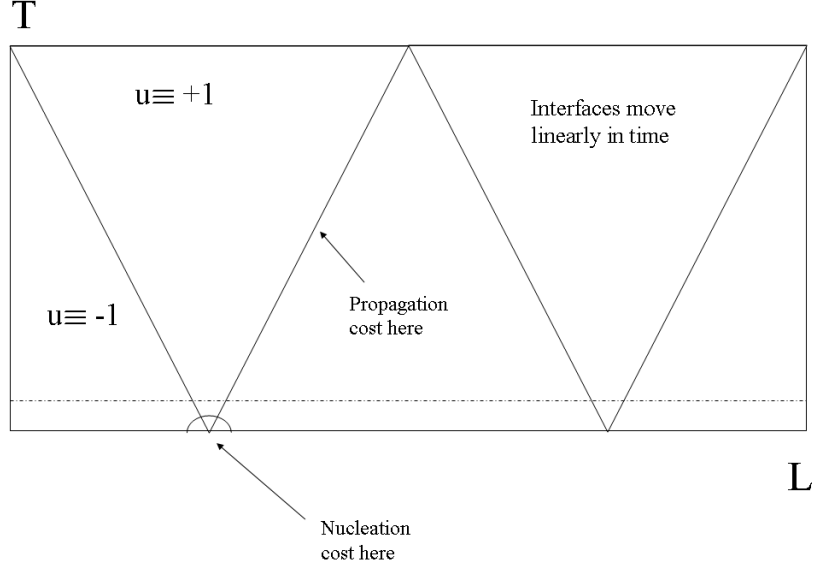


Figure 3: Action minimizer for  $L = 8\sqrt{T}$ .

### Overview of the five stages

**Stage 1.** In time  $T_0$ , linearly interpolate from  $u \equiv -1$  to  $u_0$ , a point on the orbit connecting (in infinite time)  $u_n$  with  $u \equiv -1$  under the dynamics  $\dot{u} = u_{xx} - V'(u)$ . (As long as  $L_1 < \tilde{L}/2$ ,  $u_n$  is in the basin of attraction of  $u \equiv -1$ , so this orbit exists. Actually, we will choose  $L_1 < \tilde{L}/4$  for (3.2), below.)

**Stage 2.** In time  $T_1$ , follow the orbit from  $u_0$  to  $u_n$  with time reversed dynamics.

**Stage 3.** In time  $T_2 := T - 2T_0 - 2T_1$ , propagate the hyperbolic tangent profiles, using  $u(x, t) := v(x, t - T_1 - T_0)$ , with

$$v(x, t) := \begin{cases} \tanh\left(\frac{L_1 + x + ct}{\sqrt{2}}\right) & x \leq 0 \\ \tanh\left(\frac{L_1 - x + ct}{\sqrt{2}}\right) & x > 0, \end{cases}$$

where  $c := (\tilde{L} - 2L_1)/T_2$  so that the zeros of the tangents reach  $\pm(\tilde{L} - L_1)$  by the end of propagation.

**Stage 4.** In time  $T_1$ , follow the orbit from this state to a point arbitrarily near  $u \equiv +1$ . (This is symmetric to Stage 2, except that we follow the orbit in forward time.)



**Stage 5.** In time  $T_0$ , linearly interpolate to  $u \equiv +1$ .

**Choice of parameters and action cost**

By calculating as in (1.14), the action cost in the second stage is  $(E(u_n) - E(u_0)) \leq E(u_n)$ . The energy of  $u_n$  on each half line converges monotonically as  $L_1 \rightarrow \infty$ , which comes from calculating

$$\int_{-b}^b \frac{1}{2} (\partial_x \tanh(x/\sqrt{2}))^2 + \frac{1}{4} (1 - \tanh^2(x/\sqrt{2}))^2 dx \underset{b \rightarrow \infty}{\uparrow} \frac{2\sqrt{2}}{3},$$

(by using  $u$ -substitution with  $u(x) := \tanh(x/\sqrt{2})$  and using the identity  $u'(x) = (1 - u^2)/\sqrt{2}$ ). Therefore, the action of this stage is bounded by  $2 \times 2\sqrt{2}/3$ . Fix  $L_1$ . (When we patch the function near  $x = 0$  we will choose  $L_1 \gg 1$  to control the error.)

Now choose  $u_0$  on the orbit between  $-1$  and  $u_n$  (corresponding to the  $L_1$  chosen above) such that  $u_0$  is not identically  $-1$  and the action cost of the linear interpolation in stage one costs less than  $\delta/(4N)$ . We use the lemma of Faris and Jona-Lasinio [12]:

**Lemma 1 (Faris and Jona-Lasinio).** *For the linear interpolant*

$$u(t) := u(a)(1 - t/\tau) + u(b)t/\tau$$

*with  $u(a)$  and  $u(b)$  uniformly bounded and  $\|D_u E[u(a)]\|_{L^2} < \infty$ ,  $\|D_u E[u(b)]\|_{L^2} < \infty$ , there exists a constant  $c < \infty$  and a  $T_0 \in (0, \infty)$  such that the corresponding  $u$  satisfies*

$$S_{[0, T_0]}[u] \leq 2c \|u(a) - u(b)\|_{L^2}.$$

The proof is by separating the action as in (1.17). The time derivative is controlled by

$$\frac{\|u(a) - u(b)\|_{L^2}^2}{\tau}$$

and  $\|D_u E[u(t)]\|_{L^2}$  is estimated in terms of the end states plus a bounded function, so that the second term in (1.17) is bounded by

$$C\tau.$$

Optimizing on  $\tau$  completes the proof. By the lemma, it is possible to interpolate with a low cost, and there is a corresponding (small and finite) time  $T_0$  which is optimal.

Next, find the time  $T_1$  needed to connect states  $u_n$  and  $u_0$ . Note that  $T_1$  is finite but large. According to a theorem of Carr and Pego [4],  $T_1 \approx e^{2\sqrt{2}L_1}$ .

Finally, consider the action for the propagation phase, Stage 3. Here, the propagation action on each cell is bounded by

$$\begin{aligned} \frac{\sqrt{2}}{3} c^2 T_2 &= \frac{\sqrt{2}}{3} \left( \frac{\tilde{L} - 2L_1}{T_2} \right)^2 T_2 \\ &= \frac{\sqrt{2}}{3} \frac{(\tilde{L} - 2L_1)^2}{T_2} \\ &\leq \frac{\sqrt{2}}{3} \frac{\tilde{L}^2}{T - 2T_0 - 2T_1} \\ &= \frac{\sqrt{2}}{12} \frac{L^2/N^2}{T - 2T_0 - 2T_1}, \end{aligned}$$

for  $\tilde{L} \geq 2L_1$ . Thus, multiplying by  $N$ , the total propagation action for  $T^*$  sufficiently large satisfies the bound

$$\begin{aligned} S_{[T_0+T_1, T-(T_0+T_1)]}[u] &\leq \frac{\sqrt{2}}{12} \frac{L^2}{NT} (1 - 2(T_0 + T_1)/T)^{-1} \\ &\leq \frac{\sqrt{2}}{12} \frac{L^2}{NT} + \frac{\delta}{4}. \end{aligned}$$

Now for any  $T \geq T^*$ , let  $u$  be constructed as outlined, with the given choices for  $u_0$ ,  $T_0$ ,  $L_1$ , and  $T_1$ . Then the total action

$$\begin{aligned} S_{[0, T]}[u] &\leq \frac{\delta}{4} + \frac{4\sqrt{2}}{3} N + \left( \frac{\sqrt{2}}{12} \frac{L^2}{NT} + \frac{\delta}{4} \right) + \frac{\delta}{4}, \\ &\leq \frac{4\sqrt{2}}{3} N + \frac{\sqrt{2}}{12} \frac{L^2}{NT} + \delta \\ &= \left( 2N + \frac{L^2}{8NT} \right) c_0 + \delta. \end{aligned}$$

Minimizing over  $N$  completes the argument.

### Smoothing the discontinuity

We now return to the discontinuity in the derivative of the test function at  $x = 0$ , which we have ignored. We use the fact that the discontinuity vanishes as  $L_1 \rightarrow \infty$ . Consider a smooth function  $\phi : \mathbb{R} \rightarrow \mathbb{R}$  such that  $\phi(x) \equiv 1$  for  $x \leq -1$ ,  $\phi(x) \equiv 0$  for  $x \geq 1$  and  $\phi$  and its derivatives are bounded by 1. Define the smooth nucleation state:

$$\tanh\left(\frac{x + L_1}{\sqrt{2}}\right) \phi\left(\frac{x}{a}\right) + \tanh\left(\frac{-x + L_1}{\sqrt{2}}\right) \left(1 - \phi\left(\frac{x}{a}\right)\right),$$

for a small constant  $a$ . We now show that the estimate for the cost of the action in Stage 2 remains valid. Let  $\mathcal{E}u := (\partial_x u)^2/2 + (1 - u^2)^2/4$ . Then

$$E(u_n) = \int_{-\tilde{L}}^{-a} \mathcal{E} \left( \tanh \left( \frac{x + L_1}{\sqrt{2}} \right) \right) dx + \int_a^{\tilde{L}} \mathcal{E} \left( \tanh \left( \frac{-x + L_1}{\sqrt{2}} \right) \right) dx + \int_{-a}^a \mathcal{E}(u_n) dx.$$

The first two integrals are bounded by  $2\sqrt{2}/3$  as before, and the last integral vanishes as  $a \rightarrow 0$  by virtue of the fact that

$$|\tanh((x + L_1)/\sqrt{2}) - \tanh((-x + L_1)/\sqrt{2})| \leq C|x|$$

for  $x \in [-a, a]$ .

In Stage 3 we let

$$v(x, t) := \tanh \left( \frac{x + L_1 + ct}{\sqrt{2}} \right) \phi \left( \frac{x}{a} \right) + \tanh \left( \frac{-x + L_1 + ct}{\sqrt{2}} \right) \left( 1 - \phi \left( \frac{x}{a} \right) \right).$$

We need to check the behavior of the action for  $x \in [-a, a]$ . The bound on the propagation term on this interval holds as before. To deal with the other term, we use  $(u_{xx} + u - u^3)^2 \leq 2u_{xx}^2 + 2(u - u^3)^2$ . For the  $u - u^3$  term, notice that  $u$  is a convex combination of the values of the two hyperbolic tangents, and on  $[-a, a]$ ,

$$1 \geq u \geq \tanh \left( \frac{L_1 - 1 + ct}{\sqrt{2}} \right) =: 1 - \delta.$$

To complete the bound, we will also need to bound the wall speed from below. To this end, recall the definition

$$c := \frac{\tilde{L} - 2L_1}{T_2},$$

and the relationships  $L_1 \leq \tilde{L}/4$ ,  $\hat{L} = L/2N$ , and  $N \sim L/\sqrt{T}$ . We estimate

$$c \geq \frac{\tilde{L}}{2T_2} \geq \frac{\tilde{L}}{2T} = \frac{L}{4NT} \gtrsim \frac{1}{\sqrt{T}}. \quad (3.2)$$

With these estimates in hand,

$$\begin{aligned} 2 \int_{T_0+T_1}^{T-T_0-T_1} \int_{-a}^a (u - u^3)^2 dx &\leq 2 \int_0^T \int_{-a}^a (4\delta)^2 dx dt \quad (\text{for } \delta \text{ sufficiently small}) \\ &\lesssim a \int_0^T e^{-2\sqrt{2}(L_1-1+ct)} dt \\ &\lesssim \frac{ae^{-2\sqrt{2}L_1}}{c} \\ &\lesssim ae^{-2\sqrt{2}L_1} \sqrt{T}. \end{aligned}$$

We control this term by choosing  $\sqrt{T} \ll e^{2\sqrt{2}L_1}$ . Note that since increasing  $L_1$  forces an exponential increase in  $T_1$  (as  $e^{2\sqrt{2}L_1}$ ), it is critical that we can satisfy  $T^{1/2} \ll T_1 \ll T$ . As this is no problem for  $T \rightarrow \infty$ , given any  $\delta$ , choosing  $T^*$  large enough suffices to secure the estimates.

Finally, consider the  $u_{xx}^2$  term. On  $[-a, a]$ ,  $u_{xx}$  is a rather long expression which we refrain from writing in full, but the worst term is the one in which both derivatives fall on  $\phi$ , which we bound in the following way

$$\begin{aligned}
& \int_0^{T_2} \int_{-a}^a \left| a^{-2} \phi'' \left( \frac{x}{a} \right) \left( \tanh \left( \frac{x + L_1 + ct}{\sqrt{2}} \right) - \tanh \left( \frac{-x + L_1 + ct}{\sqrt{2}} \right) \right) \right|^2 dx dt \\
& \leq a^{-4} \int_0^{T_2} \int_{-a}^a \left| \tanh \left( \frac{x + L_1 + ct}{\sqrt{2}} \right) + \tanh \left( \frac{x - L_1 - ct}{\sqrt{2}} \right) \right|^2 dx dt \\
& \leq 2a^{-4} \int_0^{T_2} \operatorname{sech}^4 \left( \frac{L_1 - 1 + ct}{\sqrt{2}} \right) \int_{-a}^a x^2 dx dt \\
& = \frac{4a^{-1}}{3} \int_0^{T_2} \operatorname{sech}^4 \left( \frac{L_1 - 1 + ct}{\sqrt{2}} \right) dt \\
& \leq \frac{64a^{-1}}{3} \int_0^{T_2} e^{-2\sqrt{2}(L_1 - 1 + ct)} dt \\
& = \frac{64a^{-1} e^{-2\sqrt{2}(L_1 - 1)}}{6\sqrt{2}c} \left( 1 - e^{-2\sqrt{2}cT_2} \right) \\
& \lesssim \frac{a^{-1}}{c} e^{-2\sqrt{2}L_1} \\
& \lesssim \frac{T^{1/2}}{a} e^{-2\sqrt{2}L_1}.
\end{aligned}$$

As before, we control this term by choosing  $L_1$  sufficiently large.  $\square$

### 3.2 Higher space dimensions

The  $\Gamma$ -limit candidates (2.1) and (2.3) tell us how minimizers of (1.10) behave for small  $\varepsilon$ , guiding our development of upper bound constructions. In one space dimension, it is straightforward to solve the limit problem posed by (2.3), but the reduced functional in  $d > 1$  is more complicated to analyze. Below, we use it to develop two very different classes of candidates for upper bound constructions in  $d > 1$ , both of which give the same scaling law. The first class are one-dimensional constructions. The second class are the MCF-based constructions, built around the mean-curvature-flow skeleton of Section 2. In some sense, it is surprising that one-dimensional constructions can compete with MCF-based constructions, which take advantage of the ge-

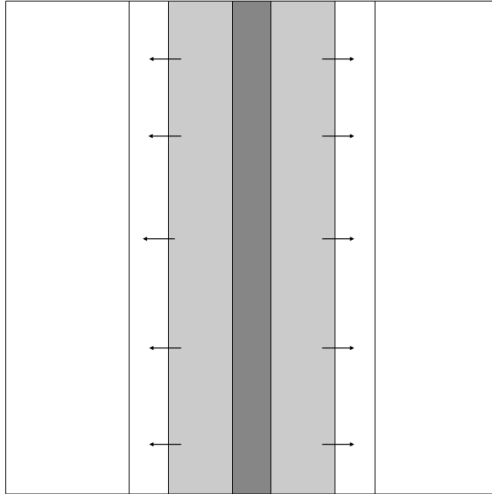


Figure 4: The stripe pattern, a one-dimensional construction for periodic boundary conditions.

ometric freedom and deterministic dynamics associated with higher dimensions. Indeed, in Subsection 3.2.4, we show that at least for  $d = 2$ , accelerated mean-curvature-flow beats the one-dimensional constructions. In other words, action minimizers *must* involve two-dimensional structure. We expect that the behavior is generic for any  $d \geq 2$ ; namely, that while one-dimensional constructions can achieve the optimal action in the energy-barrier regime, higher dimensional constructions are necessary in the sharp-interface limit.

If we assume that the action minimizing front is monotone, we can rewrite the second term in (1.12) in terms of  $\phi(x)$ , the arrival time of the front at position  $x$ :

$$\frac{c_0}{4} \int_{\Omega} |\nabla\phi| \left( \frac{1}{|\nabla\phi|} + \nabla \cdot \frac{\nabla\phi}{|\nabla\phi|} \right)^2 dx. \quad (3.3)$$

Using (1.12) or (3.3) to study the full problem is in some sense the opposite of a current method in image processing, in which a sharp-interface problem is analyzed by studying a diffuse-interface approximation. See, for instance, [2, 5, 10].

### 3.2.1 One-dimensional constructions

**Proposition 3 (Upper bound, one-dimensional constructions).** *For periodic boundary conditions and  $d > 1$ , the action satisfies*

$$\limsup_{\varepsilon \rightarrow 0} \hat{S}_{switch} \leq \min_{N \in \mathbb{N}} \left( 2N + \frac{L^2}{8NT} \right) c_0 L^{d-1}.$$

*Proof.* We use the same construction as for  $d = 1$ , replacing the nucleation points with  $(d - 1)$ -dimensional hyperplanes (which propagate as travelling planes).  $\square$

**Corollary 3.** *For Neumann boundary conditions and  $d > 1$ ,*

$$\limsup_{\varepsilon \rightarrow 0} \hat{S}_{switch} \leq \min_{N \in \mathbb{N}} \left( N + \frac{L^2}{4NT} \right) c_0 L^{d-1}.$$

### 3.2.2 Connection with curvature flow

The reduced action functional (2.1) suggests curvature flow. Indeed, as the sharp-interface analogue of (1.16), consider constructions of interface functions which are built out of point nucleations plus reverse and forward curvature flow to an intermediate state on the ridge, i.e.  $\Gamma(T^*) = g$  and

$$v_n = \begin{cases} +\kappa & 0 \leq t \leq T^* \\ -\kappa & T^* < t \leq T. \end{cases} \quad (3.4)$$

Point nucleations incur no nucleation cost. Moreover, the calculation

$$\begin{aligned} S^R[\Gamma(\cdot)] &\geq \frac{c_0}{4} \int_0^{T^*} \int_{\Gamma(t)} \left( (v_n - \kappa)^2 + 4\kappa v_n \right) d\sigma dt \\ &\geq \frac{c_0}{4} \int_0^{T^*} \int_{\Gamma(t)} (4\kappa v_n) d\sigma dt \\ &= \frac{c_0}{4} \int_0^{T^*} 4\dot{P}(\Gamma(t)) dt \\ &= c_0 P(g), \end{aligned}$$

shows that (3.4) leads to an action cost which is equal to the perimeter of  $g$ , and no other construction passing through  $g$  can do better. This suggests the time-dependent perimeter problem:

*What is the state with minimal perimeter which can be reached by forward and reverse curvature flow in time  $T/2$ ?*

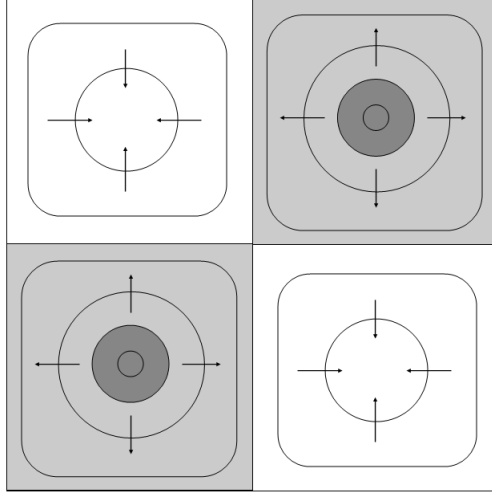


Figure 5: Sketch of an MCF construction. Reverse curvature motion carries the interface from two point nucleations to two gray squares. After the checkerboard is complete, the white squares collapse by forward curvature flow.

Note that we have not actually reduced the action minimization problem to a perimeter problem, because we have only demonstrated optimality among states which can be reached, in time, by curvature flow. In all likelihood, the optimal path accelerates or otherwise modifies its motion so that it can pass through an energetically better state, in exchange for a nonzero propagation cost. These ideas generate the MCF-based upper bound constructions and accelerated curvature flow constructions below.

### 3.2.3 MCF-based constructions

For MCF-based constructions, we choose  $g$  to be a “checkerboard state” of appropriate scale, and apply (3.4), as illustrated in Figure 5. The interfaces  $\Gamma(t)$  serve as the zero level sets of the constructions. Proposition 4 demonstrates that the MCF-based constructions satisfy the optimal action scaling law,  $S[u] \sim L^d/\sqrt{T}$  (cf. the introduction and Appendix A).

**Proposition 4 (Upper bound, MCF-based constructions).**

*For  $d > 1$ , it is possible to achieve the optimal scaling of the action functional,*

$$\limsup_{\varepsilon \rightarrow 0} \hat{S}^\varepsilon[u] \sim \frac{L^d}{\sqrt{T}},$$

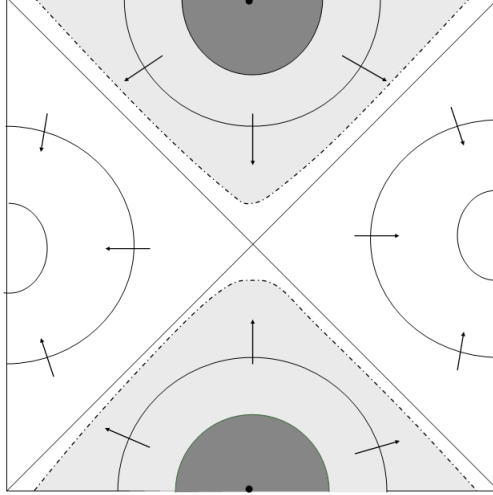


Figure 6: The cross pattern, an MCF construction for periodic boundary conditions.

*via constructions which use MCF flow on the natural, deterministic timescale.*

*Proof.* The backbone of the construction is identification of the interface,  $\Gamma(t)$ , which defines the zero level set of our test functions:

$$u_\varepsilon(x, t) := \tanh\left(\frac{d(x, \Gamma(t))}{\varepsilon\sqrt{2}}\right).$$

We create the interface at time  $0 < t' \ll 1$ , with  $\Gamma(t')$  a finite collection of points. We need to connect  $u_\varepsilon(x, t')$  to the initial state  $u_\varepsilon(x, 0) \equiv -1$ , and count the action on  $[0, t']$  separately. However, since  $\Gamma(t')$  is comprised of only finitely many points,  $\hat{E}^\varepsilon[u_\varepsilon(\cdot, t')] \xrightarrow{\varepsilon \rightarrow 0} 0$ , and consequently, we can connect the states with negligible action cost.

Let  $\ell$  be the largest possible value such that  $[0, \ell]^d$  collapses by MCF in time  $t = T/2$ . (The length-scale  $\ell$  scales like  $\sqrt{T}$ .) Since we are only interested in the scaling, we assume for simplicity that  $L/\ell \in \mathbb{N}$ . To construct  $\Gamma(t)$ , break the system into  $n = (L/\ell)^d$  periodic cells so that on each cell, there is sufficient time to follow the reverse MCF path from a point to a square. To proceed, consider a checkerboard overlay of the system. A four square checkerboard is sketched in Figure 5. On the “black” squares, let  $\Gamma(0)$  be the center of the square, and  $\Gamma(T/2)$  be the perimeter of the square. For  $t \in [0, T/2]$ , let the interface move by reverse mean-curvature-flow from the initial to final state.



Thus, at  $t = T/2$ , the interface has grown to the outline of the checkerboard. For  $t \in [T/2, T]$ , let the interface relax from this state to the centers of the “white” squares by forward curvature motion.

Since we use the deterministic motion, the limiting action cost is just the perimeter of the “checkerboard state” with  $n$  cells (cf. Subsection 3.2.2):

$$\lim_{\varepsilon \rightarrow 0} \hat{S}^\varepsilon[u_\varepsilon] = c_0 P = \frac{d c_0 L^d}{\ell} \sim \frac{L^d}{\sqrt{T}}.$$

□

**Remark 2.** *Under periodic boundary conditions, the smallest checkerboard reduces to a cross pattern (Figure 6), where two point nucleations at a pair of parallel edges introduce growing interfaces. Since the energy barrier of the cross is higher than that of the one-dimensional stripe, the stripe achieves a lower action than the cross in the energy barrier regime. In the sharp-interface limit, however, curvature based constructions are competitive; see below.*

**Remark 3.** *Our checkerboard construction “is in no hurry.” If the interface were to move faster than the natural timescale, it could go through a coarser, energetically favored checkerboard, at the expense of a propagation cost. We use this idea in the following proposition for dimension  $d = 2$ .*

### 3.2.4 Accelerated curvature flow

In  $d = 2$ , we know the precise timescale for curvature motion. We use this knowledge to show that accelerated curvature flow (checkerboards with  $v_n = \gamma\kappa$ ) can beat one-dimensional constructions in the sharp-interface regime. We do not claim that this is the optimal construction, but it shows that the optimal path must have two-dimensional structure. (This is *not* true in the energy-barrier regime.)

**Proposition 5 (A more precise upper bound for  $d = 2$ ).** *For periodic boundary conditions and dimension  $d = 2$ , it is possible to use accelerated MCF to derive the improved upper bound*

$$\limsup_{\varepsilon \rightarrow 0} \hat{S}_{switch} \leq \min_{N \in \mathbb{N}} \left( \frac{(2N)^3 \pi T}{L^2} + \frac{L^4}{2N \pi^2 T} \right) c_0 L. \quad (3.5)$$

*Proof.* We work in terms of the interface,  $\Gamma(t)$ , and use an  $N \times N$  checkerboard as in the previous proposition. Let the normal velocity of the interface be a constant multiple of the curvature,  $v_n = \pm\gamma\kappa$  for some  $\gamma > 0$ . We will choose

the constant  $\gamma = \gamma(N)$  so that the checkerboard is reached in exactly time  $T/2$ . For any closed, planar curve,

$$\dot{A}(t) = \int_{\Gamma(t)} v_n = - \int_{\Gamma(t)} \gamma \kappa = -\gamma \int_{\Gamma(t)} \frac{d\theta}{d\sigma} d\sigma = -2\pi\gamma,$$

where  $A(t)$  is the area enclosed by the curve  $\Gamma(t)$  and  $\theta$  is the angle between a point on the curve and a fixed axis. Therefore, we impose

$$\ell^2 = \pi\gamma T \Rightarrow \gamma = \frac{\ell^2}{\pi T} = \frac{L^2}{\pi T N^2}. \quad (3.6)$$

We calculate the cost in the reduced action functional, for the growth phase:

$$\begin{aligned} \frac{c_0}{4} \int_0^{T/2} \int_{\Gamma(t)} (v_n + \kappa)^2 d\sigma dt &= \frac{c_0}{4} (1 + \gamma)^2 \int_0^{T/2} \int_{\Gamma(t)} \kappa^2 d\sigma dt \\ &= \frac{c_0}{4} \frac{(1 + \gamma)^2}{\gamma} \int_0^{T/2} \int_{\Gamma(t)} \kappa v_n d\sigma dt \\ &= \frac{c_0}{4} \frac{(1 + \gamma)^2}{\gamma} P(T/2) \\ &= \frac{c_0}{4} \frac{(1 + \gamma)^2}{\gamma} 2NL, \end{aligned}$$

and similarly for the collapse phase:

$$\frac{c_0}{4} \int_{T/2}^T \int_{\Gamma(t)} (v_n + \kappa)^2 d\sigma dt = \frac{c_0}{4} \frac{(1 - \gamma)^2}{\gamma} 2NL.$$

(In particular, choosing  $v_n = \kappa$  accrues no cost for the collapse phase. The optimal  $n$  typically requires  $\gamma > 1$ , however, since that allows for a smaller perimeter.) Adding the costs, substituting for  $\gamma$  from (3.6), and keeping in mind the periodicity requirement leads to (3.5).  $\square$

If we minimize over  $N \in \mathbb{R}$ , we find that the action for the MCF constructions does slightly better (by a factor of .99) than the one-dimensional constructions. It also does slightly better when minimizing over integers, for a wide range of the parameter  $L/\sqrt{T}$ .

## 4 Lower bounds

We begin by developing the rough lower bound  $\hat{S}_{switch} \geq L^d/(3\sqrt{T})$ , for arbitrary dimension. An ansatz-free, tight lower bound requires more work and

relies on the limiting behavior of the energy measures. In Subsection 4.2, we illustrate the role of the energy by demonstrating how two hypotheses on the energy (reasonable for action minimizers) and an elementary argument lead to the improved 1-d lower bound

$$\liminf_{\varepsilon \rightarrow 0} \hat{S}_{switch} \geq c_0 \frac{L}{\sqrt{T}}. \quad (4.1)$$

This bound is sharp (i.e. it matches the upper bound) when  $L/(4\sqrt{T}) \in \mathbb{N}$ . In Subsection 4.3, we consider what is necessary for a rigorous proof.

## 4.1 Scaling bound

**Proposition 6 (Lower bound scaling).** *For all functions  $u$  with*

$$u(x, 0) \equiv -1 \quad \text{and} \quad u(x, T) \equiv +1$$

*(with periodic or Neumann boundary conditions), the action functional satisfies*

$$\hat{S}^\varepsilon[u] \geq \frac{1}{3} \frac{L^d}{\sqrt{T}}.$$

*Proof.* On the one hand, letting  $E(t) := \hat{E}^\varepsilon[u(\cdot, t)]$ ,

$$\hat{S}^\varepsilon[u] \geq \max_{0 \leq t \leq T} E(t) \geq \frac{1}{T} \int_0^T E(t) dt \geq \frac{1}{T} \int_0^T \int_{\Omega_L} \frac{(1-u^2)^2}{4\varepsilon} dx dt. \quad (4.2)$$

On the other hand,

$$\hat{S}^\varepsilon[u] \geq \frac{1}{4} \int_0^T \int_{\Omega_L} \varepsilon \dot{u}^2 dx dt .$$

Combining these inequalities,

$$\begin{aligned} \hat{S}^\varepsilon[u] &\geq \frac{1}{2} \left( \frac{1}{4} \int_0^T \int_{\Omega_L} \varepsilon \dot{u}^2 dx dt + \frac{1}{T} \int_0^T \int_{\Omega_L} \frac{(1-u^2)^2}{4\varepsilon} dx dt \right) \\ &\geq \frac{1}{4} \left( \int_0^T \int_{\Omega_L} \dot{u}^2 dx dt \right)^{1/2} \left( \frac{1}{T} \int_0^T \int_{\Omega_L} (1-u^2)^2 dx dt \right)^{1/2} \\ &\geq \frac{1}{4\sqrt{T}} \int_0^T \int_{\Omega_L} |\dot{u}(1-u^2)| dx dt \\ &= \frac{1}{4\sqrt{T}} \int_{\Omega_L} \int_0^T |\dot{u}(1-u^2)| dt dx \\ &\geq \frac{L^d}{3\sqrt{T}}. \end{aligned}$$

□

## 4.2 Sharp 1-d bound, under two assumptions

We derive the improved bound (4.1) under the hypotheses that aside from a small initial and final layer in time, the energy is approximately constant, and that there is approximate equipartition of energy. The hypotheses are natural in dimension one. To achieve switching, the function *must* form interfaces. Since there is no advantage for walls to nucleate late or disappear early, we expect the number of walls to remain fixed. The  $D_u \hat{E}^\varepsilon$  term in (1.10) drives the interfaces towards the optimal profile. Thus, in one dimension, we expect an approximately constant energy and approximate equipartition as the walls propagate.

**Proposition 7 (Tight lower bound, with assumptions).** *Let  $u_\varepsilon : [0, L] \rightarrow \mathbb{R}$  be a sequence of smooth functions which satisfy periodic or Neumann boundary conditions and  $u_\varepsilon(x, 0) \equiv -1$  and  $u_\varepsilon(x, T) \equiv +1$ . Suppose that the following two assumptions also hold as  $\varepsilon \rightarrow 0$ .*

1. *There are times  $T' = o(1)$ ,  $T'' = T - o(1)$ , such that*

$$E(T') = E(T'') = \max_{0 \leq t \leq T} E(t) + o(1).$$

2. *On  $[T', T'']$ , we have approximate equipartition of energy, i.e.*

$$\frac{1}{2} \int_{\Omega_L} \varepsilon (u_{\varepsilon, x})^2 dx = \int_{\Omega_L} \frac{V(u_\varepsilon)}{\varepsilon} dx + o(1).$$

*Then:*

$$\liminf_{\varepsilon \rightarrow 0} \hat{S}^\varepsilon[u_\varepsilon] \geq c_0 \frac{L}{\sqrt{T}}.$$

*Proof.* Taking the limit on the sequence is necessary only to remove the  $o(1)$  terms. Therefore, in the following calculations, we fix  $\varepsilon$  and omit the subscript on the function  $u$ . Define

$$E_{max} := \max_{0 \leq t \leq T} E(t).$$

We split the action over  $[0, T']$  and  $[T', T'']$ . On the first interval, there is a nucleation cost which comes from the jump in energy:

$$\hat{S}_{[0, T']}^\varepsilon[u] \geq E_{max} + o(1).$$

On the second interval, there is a propagation cost from the motion of the interfaces. To estimate the cost, we introduce the following lemma.

**Lemma 2 (Control in time).** *Let*

$$I(t) := \int_0^L (u - u^3/3)(\cdot, t) dx.$$

*We have the estimate*

$$|I(t) - I(s)| \leq C|t - s|^{1/2}.$$

*Proof.* We combine the action and energy bounds

$$\begin{aligned} |I(t) - I(s)| &= \left| \int_s^t \int_0^L \dot{u}(1 - u^2) dx dt' \right| \\ &\leq \left( \int_s^t \int_0^L \varepsilon \dot{u}^2 dx dt' \right)^{1/2} \left( \int_s^t \int_0^L \frac{(1 - u^2)^2}{\varepsilon} dx dt' \right)^{1/2} \\ &\leq C|t - s|^{1/2}. \end{aligned}$$

□

Lemma 2 and the initial and final conditions imply:

$$J := \int_{T'}^{T''} \int_0^L \dot{u}(1 - u^2) dx dt = \frac{4}{3}L + o(1). \quad (4.3)$$

On the other hand,

$$J \leq \left( \int_{T'}^{T''} \int_0^L \varepsilon \dot{u}^2 dx dt \right)^{1/2} \left( \int_{T'}^{T''} \int_0^L \frac{(1 - u^2)^2}{\varepsilon} dx dt \right)^{1/2}.$$

The idea is to use the  $\iint \varepsilon \dot{u}^2 dx dt$  term to estimate the propagation cost. We have

$$\begin{aligned} &\frac{1}{4} \int_{T'}^{T''} \int_0^L \left( \varepsilon^{1/2} \dot{u} + \varepsilon^{-1/2} D_u \hat{E}^\varepsilon(u) \right)^2 dx dt \\ &= \frac{1}{4} \int_{T'}^{T''} \int_0^L \varepsilon \dot{u}^2 + \varepsilon^{-1} D_u \hat{E}^\varepsilon(u)^2 dx dt + \frac{1}{2} (E(T'') - E(T')) \\ &\geq \frac{1}{4} \int_{T'}^{T''} \int_0^L \varepsilon \dot{u}^2 dx dt, \end{aligned}$$

where the energy difference vanishes by the hypothesis on  $T'$  and  $T''$ . Therefore,

$$\begin{aligned}
J &\leq 2 (S_{[T',T'']}[u])^{1/2} \left( \int_{T'}^{T''} \int_0^L \frac{(1-u^2)^2}{\varepsilon} dx dt \right)^{1/2} \\
&\leq 2 (S_{[T',T'']}[u])^{1/2} \left( 2 \int_{T'}^{T''} E(t) + o(1) dt \right)^{1/2} \quad (\text{by equipartition}) \\
&\leq 2\sqrt{2T} (S_{[T',T'']}[u])^{1/2} (E_{max} + o(1))^{1/2}. \tag{4.4}
\end{aligned}$$

Combining (4.3) and (4.4),

$$S_{[T',T'']}[u] \geq \frac{2}{9} \frac{L^2}{TE_{max}} + o(1).$$

Thus,

$$\begin{aligned}
S[u] &\geq \min_M \left( M + \frac{2}{9} \frac{L^2}{TM} \right) + o(1) \\
&\geq \frac{2\sqrt{2}}{3} \frac{L}{\sqrt{T}} + o(1).
\end{aligned}$$

Taking the limit on the sequence of functions completes the proof.  $\square$

### 4.3 Ansatz-free bounds and equipartition of energy

A rigorous proof requires an analysis of the weak convergence of the energy measures and the limiting equipartition of energy. This is related to work of Hutchinson and Tonegawa [19] and Tonegawa [38], who study energy-bounded sequences for which

$$f_\varepsilon := \varepsilon \Delta u_\varepsilon + \varepsilon^{-1} (u_\varepsilon - u_\varepsilon^3) \tag{4.5}$$

is a bounded sequence of constants, or a sequence of functions which is bounded in  $W^{1,d}$ . They prove that the density of the limiting energy measures has integer multiplicity almost everywhere (modulo  $c_0$ ), and equipartition of energy is achieved in the limit. The analytical challenge in our setting is to extend these results under the weaker bound

$$\varepsilon^{-1} \int_0^T \int_\Omega f_\varepsilon^2 dx dt \leq C.$$

This is carried out in dimension  $d = 1$  in [21].

In this subsection, our goal is to demonstrate that the key ingredients for the lower bound on the action functional are the convergence of the energy measures and the limiting equipartition of energy. We show that provided the interface of the limit function,  $\Gamma(t) := \partial\{u_0 = 1\}$ , is sufficiently smooth and we have the convergences:

(i) Convergence of the energy measures:

$$\left( \frac{\varepsilon |\nabla u_\varepsilon|^2}{2} + \frac{V(u_\varepsilon)}{\varepsilon} \right) dx dt \rightharpoonup c_0 \mathcal{H}^{(d-1)} \llcorner \Gamma(t) dt =: \mu, \quad (4.6)$$

(ii) Limiting equipartition of energy, or vanishing of the discrepancy measures:

$$\left| \frac{\varepsilon |\nabla u_\varepsilon|^2}{2} - \frac{V(u_\varepsilon)}{\varepsilon} \right| dx dt \rightharpoonup 0, \quad (4.7)$$

then we have lower semi-continuity of the action functional in the sense that:

$$\liminf_{\varepsilon \rightarrow 0} \int_0^T \int_\Omega \varepsilon \dot{u}_\varepsilon^2 dx dt \geq c_0 \int_0^T \int_{\Gamma(t)} v_n^2 d\sigma dt, \quad (4.8)$$

$$\liminf_{\varepsilon \rightarrow 0} \int_0^T \int_\Omega \varepsilon^{-1} (\varepsilon \Delta u_\varepsilon - \varepsilon^{-1} V'(u_\varepsilon))^2 dx dt \geq c_0 \int_0^T \int_{\Gamma(t)} \kappa^2 d\sigma dt. \quad (4.9)$$

Let the set  $\mathcal{A}$  consist of all  $\zeta \in C_0^1(\Omega \times (0, T))$  such that

$$\int_0^T \int_{\Gamma(t)} \zeta^2 d\sigma dt \leq 1. \quad (4.10)$$

To show (4.8), we will use the dual representation:

$$\left( \int_0^T \int_{\Gamma(t)} v_n^2 d\sigma dt \right)^{1/2} = \sup_{\zeta \in \mathcal{A}} \int_0^T \int_{\Gamma(t)} \zeta v_n d\sigma dt. \quad (4.11)$$

Let  $A(t)$  denote the set  $\{u_0 = -1\}$ , and take the sign convention that  $n$  is the outward normal to  $A$ . We have two equalities:

$$\begin{aligned} \int_0^T \int_{\Gamma(t)} \zeta v_n d\sigma dt &= - \int_0^T \int_{A(t)} \dot{\zeta} dx dt, \\ \int_0^T \int_{\Gamma(t)} \zeta v_n d\sigma dt &= \int_0^T \int_{A^c(t)} \dot{\zeta} dx dt. \end{aligned}$$

Combining the equalities,

$$\begin{aligned}
& \int_0^T \int_{\Gamma(t)} \zeta v_n d\sigma dt \\
&= \frac{1}{2} \left( - \int_0^T \int_{A(t)} \dot{\zeta} dx dt + \int_0^T \int_{A^c(t)} \dot{\zeta} dx dt \right) \\
&= \frac{3}{4} \liminf_{\varepsilon \rightarrow 0} \left( - \int_0^T \int_{\Omega} \dot{\zeta} (u_\varepsilon - u_\varepsilon^3/3) dx dt \right) \\
&= \frac{3}{4} \liminf_{\varepsilon \rightarrow 0} \left( \int_0^T \int_{\Omega} \zeta \dot{u}_\varepsilon (1 - u_\varepsilon^2) dx dt \right) \\
&\leq \frac{3}{4} \liminf_{\varepsilon \rightarrow 0} \left( \int_0^T \int_{\Omega} \zeta^2 \frac{(1 - u_\varepsilon^2)^2}{\varepsilon} dx dt \right)^{1/2} \left( \int_0^T \int_{\Omega} \varepsilon \dot{u}_\varepsilon^2 dx dt \right)^{1/2} \\
&\stackrel{(4.6)}{=} \frac{3}{4} \left( 2c_0 \int_0^T \int_{\Gamma(t)} \zeta^2 d\sigma dt \right)^{1/2} \liminf_{\varepsilon \rightarrow 0} \left( \int_0^T \int_{\Omega} \varepsilon \dot{u}_\varepsilon^2 dx dt \right)^{1/2} \\
&\stackrel{(4.10)}{\leq} c_0^{-1/2} \liminf_{\varepsilon \rightarrow 0} \left( \int_0^T \int_{\Omega} \varepsilon \dot{u}_\varepsilon^2 dx dt \right)^{1/2}.
\end{aligned}$$

By the representation (4.11), taking the sup over  $\zeta$  implies (4.8).

Similarly, to show (4.9), we let the set  $\mathcal{A}$  consist of all  $\xi \in C_0^1(\Omega \times (0, T))^d$  such that

$$\int_0^T \int_{\Gamma(t)} |\xi|^2 d\sigma dt \leq 1, \tag{4.12}$$

and use the dual representation:

$$\left( \int_0^T \int_{\Gamma(t)} |\underline{\kappa}|^2 d\sigma dt \right)^{1/2} = \sup_{\xi \in \mathcal{A}} \int_0^T \int_{\Gamma(t)} (\xi \cdot \underline{\kappa}) d\sigma dt, \tag{4.13}$$

where  $\underline{\kappa}$  is the mean curvature vector. First, we claim that (i) and (ii) imply

$$\begin{aligned}
& \int_0^T \int_{\Omega} \left( \nabla \cdot \xi - \partial_i \xi_j \frac{\partial_i u_\varepsilon}{|\nabla u_\varepsilon|} \frac{\partial_j u_\varepsilon}{|\nabla u_\varepsilon|} \right) \varepsilon |\nabla u_\varepsilon|^2 dx dt \\
&\rightarrow c_0 \int_0^T \int_{\Gamma(t)} (\nabla \cdot \xi - \partial_i \xi_j \nu_i \otimes \nu_j) d\sigma dt \\
&= c_0 \int_0^T \int_{\Gamma(t)} (\xi \cdot \underline{\kappa}) d\sigma dt.
\end{aligned} \tag{4.14}$$

(We use a summation convention, and  $\nu$  denotes the outward unit normal to the region enclosed by  $\Gamma(t)$ .) The convergence of the first term is a direct



application of (i) and (ii). The convergence of the second term relies on the following consequence of conditions (i) and (ii), which follows from work of Reshetnyak [32]. See also Luckhaus and Modica [24]. Their results are more general; in our setting, the statement we need is:

**Proposition 8.** *Suppose conditions (i) and (ii) are satisfied. Then*

$$\varepsilon \nabla u_\varepsilon \otimes \nabla u_\varepsilon \, dx \, dt \rightharpoonup c_0 \nu \otimes \nu \mathcal{H}^{(d-1)} \llcorner \Gamma(t) dt.$$

For completeness, we include the proof.

*Proof.* Because

$$\lambda_\varepsilon := \varepsilon \nabla u_\varepsilon \otimes \nabla u_\varepsilon \, dx \, dt$$

is a bounded sequence of measures, we may assume without loss that it converges to a limit measure,  $\lambda$ . Moreover, (4.7) implies that the limiting measure  $\mu$  (defined in (4.6)) is equal to:

$$\mu = \lim_{\varepsilon \rightarrow 0} \varepsilon |\nabla u_\varepsilon|^2 \, dx \, dt.$$

Therefore,  $|\lambda| \ll \mu$  and by the Radon-Nikodym theorem, it has a representation

$$\lambda = A\mu,$$

for some  $\mu$ -measurable matrix  $A$  which is symmetric and positive semi-definite. We now study the matrix  $A$ . All of the statements which we make about  $A$  should be understood in the  $\mu$ -a.e. sense.

First of all, the calculation:

$$\mu = \lim_{\varepsilon \rightarrow 0} \varepsilon |\nabla u_\varepsilon|^2 \, dx \, dt = \lim_{\varepsilon \rightarrow 0} \text{Trace}(\varepsilon \nabla u_\varepsilon \otimes \nabla u_\varepsilon) \, dx \, dt = \text{Trace}(A) \mu,$$

reveals that

$$\text{Trace} A = 1, \tag{4.15}$$

which by the positivity of  $A$  implies in particular that the maximal eigenvalue of  $A$  is bounded by one. Thus

$$(y, A y) \leq 1, \tag{4.16}$$

for any  $y \in \mathbb{R}^d$  with  $|y| \leq 1$ . The goal is now to show that

$$(\nu, A \nu) = 1 \quad \mu - a.e., \tag{4.17}$$

which by the Rayleigh quotient implies that  $\nu$  is an eigenvector of  $A$  with eigenvalue 1. Because of (4.15) and the positivity of  $A$ ,  $\nu$  must therefore be the *only* eigenvector of  $A$  with nontrivial eigenvalue, and  $A = \nu \otimes \nu$ .

For the proof of (4.17), let  $\xi \in C_0^\infty(\Omega \times (0, T))^d$  with  $|\xi| \leq 1$  and observe:

$$\begin{aligned} \varepsilon(\xi, \nabla u_\varepsilon \otimes \nabla u_\varepsilon \xi) &= \varepsilon(\nabla u_\varepsilon, \xi)^2 = \varepsilon |\nabla u_\varepsilon|^2 \left( \frac{\nabla u_\varepsilon}{|\nabla u_\varepsilon|}, \xi \right)^2 \\ &\geq \varepsilon |\nabla u_\varepsilon|^2 \left( 2 \left( \frac{\nabla u_\varepsilon}{|\nabla u_\varepsilon|}, \xi \right) - 1 \right) \\ &= 2\varepsilon |\nabla u_\varepsilon| (\nabla u_\varepsilon, \xi) - \varepsilon |\nabla u_\varepsilon|^2, \end{aligned} \quad (4.18)$$

where to get from the first to the second line, we have used the inequality  $x^2 \geq 2x - 1$ .

We would like to integrate and pass to the limit in (4.18). The only difficult term is the first term on the r.h.s. For this term, we will use the fact that for all  $\xi$  with  $|\xi| \leq 1$ ,

$$\begin{aligned} &\iint \left| 2\varepsilon |\nabla u_\varepsilon| (\nabla u_\varepsilon, \xi) - \sqrt{2} |1 - u_\varepsilon^2| (\nabla u_\varepsilon, \xi) \right| dx dt \\ &= \iint \left| 2\varepsilon |\nabla u_\varepsilon|^2 - \sqrt{2} |1 - u_\varepsilon^2| |\nabla u_\varepsilon| \right| \left| \left( \frac{\nabla u_\varepsilon}{|\nabla u_\varepsilon|}, \xi \right) \right| dx dt \\ &\leq \iint \left| 2\varepsilon |\nabla u_\varepsilon|^2 - \sqrt{2} |1 - u_\varepsilon^2| |\nabla u_\varepsilon| \right| dx dt \\ &\leq \left( \iint \varepsilon |\nabla u_\varepsilon|^2 dx dt \iint \left( 2\sqrt{\varepsilon} |\nabla u_\varepsilon| - \sqrt{2} \frac{|1 - u_\varepsilon^2|}{\sqrt{\varepsilon}} \right)^2 dx dt \right)^{1/2} \\ &\leq \left( \iint \varepsilon |\nabla u_\varepsilon|^2 dx dt \iint \left| 4\varepsilon |\nabla u_\varepsilon|^2 - 2 \frac{(1 - u_\varepsilon^2)^2}{\varepsilon} \right| dx dt \right)^{1/2} \\ &= 2\sqrt{2} \left( \iint \varepsilon |\nabla u_\varepsilon|^2 dx dt \iint \left| \frac{\varepsilon |\nabla u_\varepsilon|^2}{2} - \frac{V(u_\varepsilon)}{\varepsilon} \right| dx dt \right)^{1/2}, \end{aligned}$$

which goes to zero by (4.7). Therefore,

$$\begin{aligned} &\lim_{\varepsilon \rightarrow 0} \int_0^T \int_\Omega 2\varepsilon |\nabla u_\varepsilon| (\nabla u_\varepsilon, \xi) dx dt \\ &= \lim_{\varepsilon \rightarrow 0} \int_0^T \int_\Omega \sqrt{2} |1 - u_\varepsilon^2| (\nabla u_\varepsilon, \xi) dx dt, \end{aligned} \quad (4.19)$$

Defining

$$W(u) := \int_0^u |1 - s^2| ds,$$

(4.19) and the convergence of  $u_\varepsilon$  to  $\pm 1$  imply

$$\begin{aligned}
& \lim_{\varepsilon \rightarrow 0} \int_0^T \int_{\Omega} 2\varepsilon |\nabla u_\varepsilon| (\nabla u_\varepsilon, \xi) \, dx \, dt \\
&= \lim_{\varepsilon \rightarrow 0} \int_0^T \int_{\Omega} \sqrt{2} (\nabla W(u_\varepsilon), \xi) \, dx \, dt \\
&= \lim_{\varepsilon \rightarrow 0} \int_0^T \int_{\Omega} -\sqrt{2} W(u_\varepsilon) (\nabla \cdot \xi) \, dx \, dt \\
&= c_0 \int_0^T \int_{A(t)} (\nabla \cdot \xi) \, dt - c_0 \int_0^T \int_{A^c(t)} (\nabla \cdot \xi) \, dt \\
&= 2c_0 \int_0^T \int_{\Gamma(t)} (\xi, \nu) \, dt \\
&= 2 \int (\xi, \nu) d\mu.
\end{aligned}$$

Therefore, integrating and taking the limit in (4.18),

$$\int (\xi, A\xi) d\mu \geq 2 \int (\xi, \nu) d\mu - \int d\mu.$$

Letting  $\xi$  approximate  $\nu$ , we conclude

$$\int (\nu, A\nu) d\mu \geq \int d\mu,$$

which, in light of (4.16), implies (4.17) and completes the proof.  $\square$

We will use the proposition together with the following identity, which we derive by multiplying (4.5) by  $\partial_j u_\varepsilon \xi_j$  and integrating by parts:

$$\begin{aligned}
& \int_0^T \int_{\Omega} \left( \nabla \cdot \xi - \partial_i \xi_j \frac{\partial_i u_\varepsilon}{|\nabla u_\varepsilon|} \frac{\partial_j u_\varepsilon}{|\nabla u_\varepsilon|} \right) \varepsilon |\nabla u_\varepsilon|^2 \, dx \, dt \\
&= \int_0^T \int_{\Omega} \left( (\nabla \cdot \xi) \left( \varepsilon \frac{|\nabla u_\varepsilon|^2}{2} - \frac{V(u_\varepsilon)}{\varepsilon} \right) + f_\varepsilon \partial_j u_\varepsilon \xi_j \right) \, dx \, dt. \quad (4.20)
\end{aligned}$$

If the sum of the first two terms on the r.h.s. vanishes in the limit by equipar-

tition of energy (cf. (4.7)), then (4.14) and (4.20) imply

$$\begin{aligned}
c_0 \int_0^T \int_{\Gamma(t)} (\xi \cdot \underline{\kappa}) \, d\sigma \, dt & \\
&= \liminf_{\varepsilon \rightarrow 0} \int_0^T \int_{\Omega} \left( \nabla \cdot \xi - \partial_i \xi_j \frac{\partial_i u_\varepsilon}{|\nabla u_\varepsilon|} \frac{\partial_j u_\varepsilon}{|\nabla u_\varepsilon|} \right) \varepsilon |\nabla u_\varepsilon|^2 \, dx \, dt \\
&= \liminf_{\varepsilon \rightarrow 0} \int_0^T \int_{\Omega} (f_\varepsilon \partial_j u_\varepsilon \xi_j) \, dx \, dt \\
&\leq \liminf_{\varepsilon \rightarrow 0} \left[ \left( \varepsilon^{-1} \int_0^T \int_{\Omega} f_\varepsilon^2 \, dx \, dt \right)^{1/2} \left( \int_0^T \int_{\Omega} \varepsilon |\nabla u_\varepsilon|^2 |\xi|^2 \, dx \, dt \right)^{1/2} \right].
\end{aligned}$$

Using (4.6) and (4.12) to bound the limit of the second term, we conclude

$$c_0 \int_0^T \int_{\Gamma(t)} (\xi \cdot \underline{\kappa}) \, d\sigma \, dt \leq \liminf_{\varepsilon \rightarrow 0} \left( \varepsilon^{-1} \int_0^T \int_{\Omega} f_\varepsilon^2 \, dx \, dt \right)^{1/2} c_0^{1/2},$$

which, together with the representation (4.13), implies (4.9).

The task of justifying hypotheses (i) and (ii) in space dimension greater than one remains a challenging open problem. The topic is linked to a conjecture of DeGiorgi, on which there has been recent progress in three space dimensions [30].

## 5 Outlook

**Relevance of short-time switching pathways.** Because the long-time switching pathway (e.g. single-nucleation pathways, in the Allen-Cahn problem) are the most likely pathways when switching is considered on its natural timescale, they receive a lot of attention. After all, on this timescale, other switching pathways are exponentially unlikely. On shorter timescales, however, different switching pathways may become relevant. In that case, estimating the probability of switching based on the long-time pathway gives a gross underestimate. This phenomenon appears, for instance, in the context of magnetic memory devices [22, 33].

**Large systems.** As discussed in the introduction, the large system limit we study here is taken *after sending the noise strength to zero*. As an example of a very different limit, consider

$$\dot{u} = u_{xx} - V'(u) + \sqrt{2\gamma} \eta, \quad x \in [-L, L],$$

where  $V$  is an *unequal* double-well potential and  $\eta$  is a space-time white noise. In that case, nucleation events are localized and the joint limit  $\gamma \rightarrow 0$  with  $L \sim \exp(c/\gamma)$  leads to multiple nucleation events which are *randomly* distributed in space and time [34].

**The sharp-interface limit of the stochastic process.** Is the limiting functional (2.3) actually the action functional for a well-defined stochastic process? Moreover, is this process the sharp-interface limit of the process defined by (1.4)? These questions involve permuting the order of the  $\varepsilon$ ,  $\gamma$  limits. Partial progress in this direction is contained in [15].

Interpreting the limiting functional (2.1) for  $d > 1$  in terms of an associated stochastic, sharp-interface problem is yet more involved, since there is also the regularization parameter,  $\lambda$ , to consider. We are not aware of work in this direction at this time.

**Boundary-vortex limit in micromagnetics.** The topic of action minimization and sharp-interface limits for stochastically perturbed partial differential equations is certainly not limited to the Allen-Cahn equation, nor is the sharp-interface limit the only interesting one. In micromagnetics, for example, one is interested in thermally-activated switching of the magnetization. There is a regime – involving submicron-scale, soft thin-films, commonly used for magnetoresistive memory devices – in which the magnetic behavior is dominated by “boundary vortices” [23, 28, 29]. We wonder whether thermally-activated switching in this regime can be described by minimizing a suitable action involving the nucleation and motion of boundary vortices.

## APPENDICES

### A Two other action regimes

We now consider two additional limiting regimes of the action (1.18): the short-time limit ( $T \rightarrow 0$ ) and the energy barrier regime ( $L, T \rightarrow \infty$  with  $L \ll \sqrt{T}$ ). See Figure 7 for an overview. As usual, we focus on periodic boundary conditions, but suitable generalization to Dirichlet or Neumann boundary conditions is usually straightforward, as we remark.

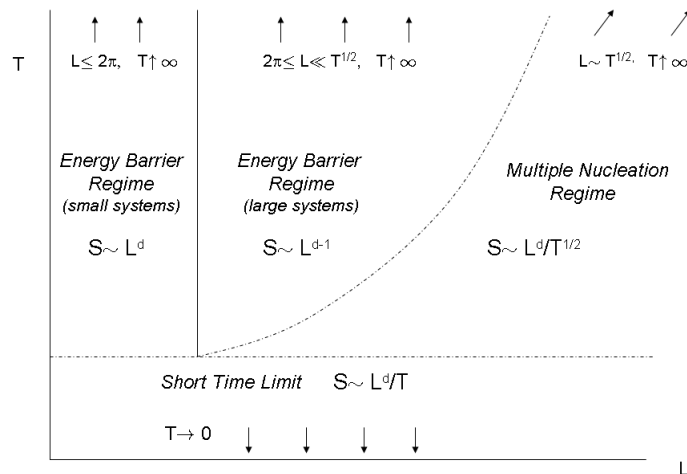


Figure 7: The scaling of the action in the four parameter regimes.

## A.1 Short-time limit

In the short-time limit ( $T \rightarrow 0$ ),

$$S_{switch} \sim \frac{L^d}{T}.$$

The heuristic here is that because time is short, the transport term  $\int_0^T \int_{\Omega_L} \dot{u}^2 dx dt$  is paramount, leading us to expect spatial independence and, to minimize the transport term, linearity in time. We prove that such a path does indeed optimize the action. The short-time limit is unique in that the optimal path completely ignores the energy landscape.

**Proposition 9 (Short time limit).** *For periodic or Neumann boundary conditions, the action satisfies*

$$\lim_{T \rightarrow 0} T S_{switch} = L^d.$$

*Proof. (Lower bound)* We show that

$$S_{switch} \geq L^d/T.$$

We use the properties of the spatial mean,  $\bar{u} := L^{-d} \int_{\Omega_L} u \, dx$ , to bound the action from below. Note that  $\bar{u}(t=0) = -1$ ,  $\bar{u}(t=T) = 1$ , and

$$\inf_{\substack{\bar{u}(0)=-1 \\ \bar{u}(T)=1}} \int_0^T \dot{\bar{u}}^2 dt = \frac{4}{T}.$$

On the other hand, Jensen's inequality gives

$$\frac{1}{L^d} \int_{\Omega_L} \dot{u}^2 dx \geq \left( \frac{1}{L^d} \int_{\Omega_L} \dot{u} dx \right)^2,$$

so that for any function  $u$  which switches in time  $T$  and obeys the boundary conditions,

$$\begin{aligned} S[u] &\geq \frac{1}{4} \int_0^T \int_{\Omega_L} \dot{u}^2 dx dt \\ &\geq \frac{L^d}{4} \int_0^T \dot{\bar{u}}^2 dt \\ &\geq \frac{L^d}{T}. \end{aligned}$$

Taking the infimum over  $u$  completes the lower bound.

**(Upper bound)** We show that

$$\limsup_{T \rightarrow 0} TS_{switch} \leq L^d.$$

We choose the spatially independent linear interpolant between end states,  $u := -1 + 2t/T$ , as a test function and compute

$$\begin{aligned} \frac{1}{4} \int_0^T \int_{\Omega_L} \dot{u}^2 + (\Delta u + u - u^3)^2 dx dt &= \frac{L^d}{4} \int_0^T \frac{4}{T^2} + (u - u^3)^2 dt \\ &= \frac{L^d}{T} (1 + O(T^2)). \end{aligned}$$

□

## A.2 Energy-barrier regime

We now switch perspectives and consider the *long-time limit* of the action. Recall that the action is always at least as big as the energy barrier. The

energy barrier regime consists of the region of parameter space in which  $T$  is taken to infinity in such a way that this bound can be achieved. According to (1.16), an action-minimizing trajectory should follow the uphill gradient flow to the minimal saddle and the downhill flow from the saddle. Although infinite time is required to complete each of the uphill and downhill journeys along the heteroclinic orbits, a switching time which is large compared to the deterministic time-scale allows a nearly optimal path to be constructed by modifying the flow near the critical points.

At first, one is surprised by the *extent* of the energy-barrier regime. The deterministic timescale for (1.3) in  $d = 1$  is exponentially large in  $L$ ; therefore, one might expect that the action is strictly larger than the energy barrier when  $L \gg \ln T$ . In fact, it is possible to achieve an action cost equal to the energy barrier even when

$$\ln T \ll L \ll \sqrt{T}.$$

To achieve the bound, we use the same constructions as for the sharp-interface limit.

In  $d > 1$ , it seems natural that  $L \sim \sqrt{T}$  marks the boundary of the energy barrier regime, since this is indeed the timescale for curvature flow. Even here, however, the sharp bound is surprising, since one-dimensional constructions are used to achieve the minimal action, and there is no apparent curvature-based construction which does as well.

We distinguish two subregions of the energy-barrier regime, according to the uniformity or nonuniformity of the minimal saddle. The crossover is at  $L = 2\pi$ , at which point the saddle  $u \equiv 0$  is supplanted by the nonuniform saddle. (The boundary condition affects the crossover point; for Neumann conditions, the transition is at  $L = \pi$ . For Dirichlet conditions, there is no small system regime, since there is only one critical point of the energy for  $L < \pi$ , and thus, no switching problem. )

### A.2.1 Energy barrier regime: small systems

In the energy barrier regime, the sharp bound (1.15) is achieved by an approximation of the pathway (1.16) through the minimal saddle. For small systems, the *only* saddle point is  $u \equiv 0$  (cf. the appendix), with energy  $L^d$ . Thus, for  $T \rightarrow \infty$  with  $L \leq 2\pi$ ,

$$S_{switch} \sim L^d.$$

As in the short-time limit, spatially uniform switching paths can be used to optimize the action, but now it is the smallness of the length scale (rather



than the time scale) which is responsible. The dynamics of the minimizing pathway are completely different from the temporally linear dynamics used for the short-time limit.

**Proposition 10 (Long time limit, small systems).** *For  $L \leq 2\pi$  and periodic boundary conditions, the action satisfies*

$$\lim_{T \rightarrow \infty} S_{switch} = \frac{L^d}{4}.$$

*Proof. (Lower bound)* For the energy-barrier regime (for both small and large systems), the lower bound comes from bounding the action by the energy of the minimum energy saddle point, as in equation (1.15). We prove in Appendix B that for  $L \leq 2\pi$ , the only saddle point is  $u_s \equiv 0$ , so the energy barrier is  $L^d/4$ .

**(Upper bound)** For the upper bound, we want to use the dynamics (1.16), modifying the flow near the critical points so that the trajectory can be following in finite time. The details of the construction are contained in the proof of the upper bound for large systems (Proposition 11, below). A difference between the construction for small and large systems is that for small systems, it suffices to use a spatially uniform switching path.  $\square$

### A.2.2 Energy barrier regime: large systems

The limit in this region is  $T \rightarrow \infty$  with  $2\pi \leq L \ll \sqrt{T}$ . We prove

$$S_{switch} \sim L^{d-1}.$$

The scaling is different for small and large systems because for  $L > 2\pi$ , the energy of the nonuniform, single-bump saddle point scales like perimeter,  $L^{d-1}$ . Our constructions based on the deterministic dynamics as in (1.16) suffice as long as

$$L \ll \ln T.$$

Notice, however, that we allow the spatial scale to grow *much faster than this*, requiring only  $L \ll \sqrt{T}$ . To achieve a bound equal to the energy barrier for

$$\ln T \ll L \ll \sqrt{T},$$

we borrow from the constructions used for the sharp-interface regime. We also use the fact that we can actually calculate the limit of the energy barrier as  $L \rightarrow \infty$  (Theorem 2 in Appendix B).

**Proposition 11.** For  $L \rightarrow \tilde{L} \in (2\pi, \infty]$  and  $T \rightarrow \infty$  with  $\limsup_{\substack{L \rightarrow \tilde{L} \\ T \rightarrow \infty}} L/\sqrt{T} \rightarrow 0$ , the action for periodic boundary conditions satisfies

$$\lim_{\substack{L \rightarrow \tilde{L} \\ T \rightarrow \infty}} S_{switch} = \Delta E(\tilde{L}), \quad (\text{A.1})$$

where  $\Delta E(\tilde{L})$  is the minimal saddle energy on an interval of length  $\tilde{L}$ .

We break the proof into two cases,  $\tilde{L} < \infty$  and  $\tilde{L} = \infty$ . The former case was already proved by Faris and Jona-Lasinio [12], but for completeness, we include both cases.

*Proof of proposition. (Lower bound)* The lower bound holds as in (1.15) for both finite and infinite  $\tilde{L}$ . (The limit of the energy barrier is well-defined even though the periodic saddle points on  $[-L, L]$  do not converge as  $L \rightarrow \infty$ . See the appendix for details.)

**(Upper bound on bounded systems)** We show that for  $\tilde{L} \in (0, \infty)$ ,

$$\limsup_{\substack{L \rightarrow \tilde{L} \\ T \rightarrow \infty}} S_{switch} \leq \Delta E(\tilde{L}).$$

By continuity, it is enough to show it for  $L$  fixed. Using Lemma 1, we construct a test function  $\tilde{u}$  in five parts. The first is a linear interpolant connecting  $u \equiv -1$  to a point arbitrarily nearby. The second follows the reversed dynamics to a point arbitrarily near the lowest energy saddle point. The third is a linear interpolant between that point and a point in the basin of attraction of  $u \equiv +1$ , also arbitrarily close to the saddle point. The fourth follows the gradient flow towards  $u \equiv +1$ . The fifth connects the endpoint of the fourth segment with  $u \equiv +1$ . By choosing  $T$  large enough, we can make the first, third, and fifth contributions to the action arbitrarily small, by the lemma. Thus,

$$\begin{aligned} \lim_{T \rightarrow \infty} S[\tilde{u}] &\leq \delta/3 + \Delta E(L) + \delta/3 + 0 + \delta/3 \\ &= \Delta E(L) + \delta. \end{aligned}$$

Letting  $\delta \rightarrow 0$ , we are done.

**(Upper bound on unbounded systems)** It is proved in the appendix that

$$\lim_{L \rightarrow \infty} L^{1-d} \Delta E(L) = 2c_0,$$

so it is enough to show

$$\limsup_{\substack{L \rightarrow \infty \\ T \rightarrow \infty}} L^{1-d} S_{switch} \leq \frac{4\sqrt{2}}{3}.$$

This inequality follows directly from the upper bound for the sharp-interface regime (Propositions 2 and 3), with one-dimensional test functions and one nucleation ( $N = 1$ ).  $\square$

**Remark 4.** *Proposition 11 also holds for Neumann boundary conditions. The only thing that changes is the value of the energy barrier.*

## B The energy and its saddle points

The purpose of this appendix is to collect relevant information about the energy and its dependence on spatial scale. The energy barrier for small systems is derived in Corollary 4 below, and the limit of the barrier for large systems is derived in Theorem 2.

**Remark 5.** *Throughout the appendix, our domain of integration is  $[0, L]^d$ .*

### B.1 Small systems

Small systems are particularly straightforward because the only periodic saddle point of the energy for  $L < 2\pi$  is  $u \equiv 0$ . This fact follows from the following theorem, which is the adaptation to periodic boundary conditions of a theorem of Gurtin and Matano [17].

**Theorem 1.** *For  $L < 2\pi$ , the only periodic critical points are constant.*

*Proof.* We use the fact that  $-1 \leq u \leq 1$ . (Suppose  $u$  has a maximum at  $x_0$  with  $u(x_0) > 1$ . Then  $\Delta u(x_0) \leq 0$  but  $(u^3 - u)(x_0) > 0$ . A similar contradiction rules out a minimum  $< -1$ .)

First, suppose  $u$  is a nonconstant critical point of one sign. Without loss, assume  $u$  is positive. Integrate the Euler-Lagrange equation, using the boundary condition to conclude

$$\int u(1 - u^2) = 0. \tag{B.1}$$

Since the integrand is positive, it must vanish, thus  $u \equiv 0$  or  $u \equiv 1$ . Similarly, if  $u$  is negative,  $u \equiv 0$  or  $u \equiv -1$ .

Now suppose that  $u$  is a nonconstant critical point which changes sign. We will obtain a contradiction by the method of Gurtin and Matano. The idea is that we want to use the smallness of the spatial domain to invoke a Poincaré inequality which contradicts an inequality supplied by the equation. The problem is the mean value which appears in the Poincaré inequality. The method around it is the following.

Since  $u$  changes sign, we can define  $w := u^+ + \alpha u^-$ , with  $\alpha > 0$  chosen such that  $\int w = 0$ . Furthermore, let  $\tilde{w} := u^+ + \alpha^2 u^-$ . Both  $w$  and  $\tilde{w}$  are periodic. They also satisfy the relations

$$\begin{aligned} u\tilde{w} &= w^2 \\ \langle \nabla u, \nabla \tilde{w} \rangle &= |\nabla w|^2. \end{aligned} \tag{B.2}$$

Hence,

$$\begin{aligned} - \int \tilde{w}(u^3 - u) &= - \int \tilde{w} \Delta u = \int \langle \nabla \tilde{w}, \nabla u \rangle \\ &= \int |\nabla w|^2 \\ &\geq \lambda \int w^2 \\ &> \int w^2, \end{aligned}$$

where  $\lambda = (2\pi/L)^2 > 1$  and no mean appears since by construction  $w$  has zero mean. On the other hand,

$$- \int \tilde{w}(u^3 - u) = - \int \tilde{w}u(u^2 - 1) \leq \int \tilde{w}u = \int w^2.$$

This contradiction establishes that there is in fact no nonconstant periodic critical point for  $L < 2\pi$ .  $\square$

**Corollary 4.** *For  $L < 2\pi$  and periodic boundary conditions, the only critical points of the energy  $E[u] = \int_{[0,L]^d} \frac{1}{2} |\nabla u|^2 + \frac{1}{4} (1 - u^2)^2 dx$  are  $u \equiv \pm 1$  and  $u \equiv 0$ . The first two are minima, the last is a saddle point.*

**Remark 6.** *As discussed earlier, the transition for Dirichlet or Neumann boundary conditions is at  $L = \pi$ , and for Dirichlet conditions, there is no switching problem for small systems since there is only one critical point.*

## B.2 The birth of a new saddle point

There is a sharp boundary at  $2\pi$  demarcating the emergence of a new, lower energy saddle point which remains the minimal saddle for all  $L \in (2\pi, \infty)$ . The bifurcation is marked by the nontrivial nullspace of the linearization of the Euler-Lagrange equation about the zero solution. We begin with a method which is specific to one dimension. While we could proceed immediately with a theorem for arbitrary dimension, the one-dimensional case allows direct calculation and builds intuition. (As noted, the transition point for Dirichlet or Neumann conditions is instead at  $\pi$ .)

Consider the Euler-Lagrange equation

$$u_{xx} = V'(u),$$

with  $V(u) := (1 - u^2)^2/4$ . Recast it as a first order system,

$$\begin{cases} u_x = p \\ p_x = V'(u), \end{cases} \quad (\text{B.3})$$

a Hamiltonian system with Hamiltonian  $H(u, p) := p^2/2 - V(u)$ .  $L$ -periodic solutions of the system satisfy

$$L = 4 \int_0^{u^*} \frac{du}{\sqrt{2(V(u) - V(u^*))}} =: f(u^*), \quad (\text{B.4})$$

where  $u^*$  is the maximum value of  $u$ .  $f(u^*)$  is monotonic increasing and

$$\lim_{u^* \rightarrow 0^+} f(u^*) = 2\pi.$$

For  $L > 2\pi$ ,  $f^{-1}(L)$  determines the unique maximum value,  $u^*$ , assumed by  $u_L$ , the unique, nontrivial, single-cycle,  $L$ -periodic solution of (B.3). Then

$$E[u_L] = -HL + 4 \int_0^{u^*} \sqrt{2(V(u) - V(u^*))} du, \quad (\text{B.5})$$

and  $H = -V(u^*)$ . We sample a range of  $u^*$  and use (B.4) and (B.5) to calculate the corresponding length and energy. Figure (8) compares the energy as a function of  $L$  of the trivial solution, the nontrivial single-cycle saddle, and the nontrivial two-cycle solution.

As  $L \rightarrow \infty$ ,  $u^* \rightarrow 1$  and the minimal saddle converges to a “kink-antikink” pair of hyperbolic tangents. The energy converges to  $4\sqrt{2}/3$ , twice the cost of a domain wall. (For Neumann conditions, the convergence is to  $2\sqrt{2}/3$ , the cost of a single wall.)

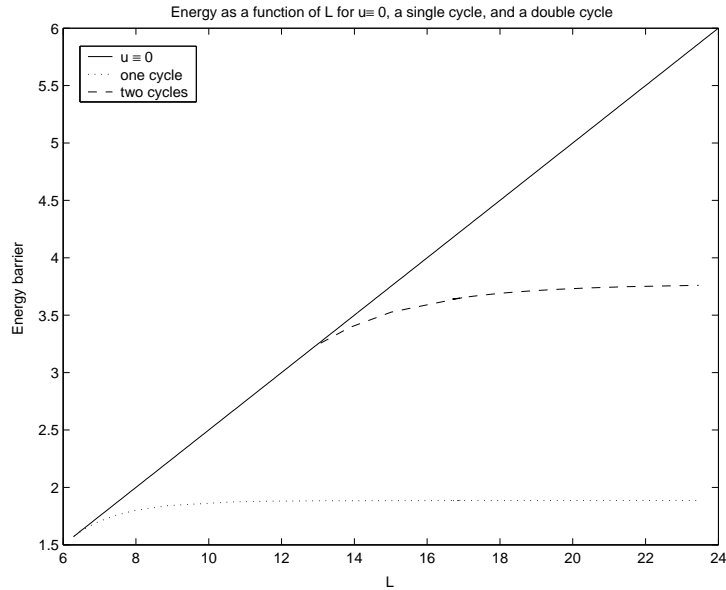


Figure 8: The energy of the saddle points vs.  $L$ .

**Remark 7.** Note that in addition, for  $L > 2n\pi$  for  $n > 1$ , there are  $n - 1$  additional nontrivial solutions, corresponding to multiple cycles. These are higher energy critical points, however. The energy of the 2-cycle saddle is illustrated in Figure 8.

### B.3 Bigger systems in higher dimensions

In higher dimensions, it remains true that a nonuniform saddle emerges as the minimal saddle. We use an elementary method to calculate the limit of the minimal saddle point energy as  $L \rightarrow \infty$  for periodic boundary conditions. (As in one dimension, the energy for Neumann conditions is half the value.)

**Theorem 2.**

$$L^{1-d}E[\text{minimal saddle}] \xrightarrow{L \rightarrow \infty} 2c_0,$$

for  $c_0 = 2\sqrt{2}/3$ .

*Proof.* By a one-dimensional construction, we have the upper bound

$$L^{1-d}E[\text{minimal saddle}] \leq c(L) \times 2 \xrightarrow{L \rightarrow \infty} 2c_0,$$

where  $2c(L)$  is the energy of the minimal periodic saddle point in one dimension. For the lower bound, a min-max argument assures

$$E[\text{minimal saddle}] \geq \min_{\bar{u}=0} E[u].$$

(There must be a mean zero state along any path from one minimizer to the other.) Therefore,

$$\begin{aligned} L^{1-d} E[\text{minimal saddle}] &\geq L^{1-d} \min_{\bar{u}=0} E[u] \\ &\xrightarrow{L \rightarrow \infty} c_0 P \\ &= 2c_0. \end{aligned}$$

Here,  $P$  denotes the minimal perimeter of a surface bounding half the volume of a periodic cube in  $d$  dimensions. The convergence follows from the result of Modica [26]. The last step uses an isoperimetric inequality of Hadwiger [18] which reveals that the minimal perimeter of a system with volume  $1/2$  on the periodic lattice is  $P = 2$ . For more about isoperimetric inequalities, see also [35].  $\square$

**Remark 8.** *The limit of the energy of the minimal saddle is achieved by one-dimensional constructions. We conjecture that for periodic boundary conditions, the minimal saddles at finite  $L$  are in fact one-dimensional.*

## Acknowledgments.

We thank Weinan E, Weiqing Ren, and Yoshi Tonegawa for their comments and insight. This paper includes and extends some of the material from the Ph.D. thesis [33]. R.V. Kohn was partially supported by NSF grants 0101439 and 0313744. F. Otto was partially supported by DFG through SFB 611. M.G. Reznikoff was partially supported by an NSF Mathematical Sciences Postdoctoral Research Fellowship. E. Vanden-Eijnden was partially supported by NSF grants DMS0101439, DMS0209959, and DMS0239625.

## References

- [1] Andrea Braides,  *$\Gamma$ -Convergence for Beginners*, Oxford University Press, Oxford, 2002.
- [2] Andrea Braides and Riccardo March, *Approximation by  $\Gamma$ -convergence of a curvature-dependent functional in visual reconstruction*, preprint.

- [3] Lia Bronsard and Robert V. Kohn, *On the slowness of phase boundary motion in one space dimension*, Comm. Pure App. Math. **43** (1990), 983–997.
- [4] J. Carr and R. L. Pego, *Metastable patterns in solutions of  $u_t = \epsilon^2 u_{xx} - f(u)$* , Comm. Pure App. Math. **42** (1989), 523–576.
- [5] Tony F. Chan, Sung Ha Kang, and Jianhong Shen, *Euler’s elastica and curvature-based inpainting*, SIAM J. Appl. Math. **63** (2002), pp. 564–592.
- [6] Giuseppe Da Prato and Jerzy Zabczyk, *Stochastic Equations in Infinite Dimensions*, Cambridge University Press, Cambridge, 1992.
- [7] Anna De Masi, Nicolas Dirr, and Errico Presutti, *Instability of interface under forced displacements*, Max-Planck-Institut für Mathematik (2005), preprint no. 5.
- [8] P. de Mottoni and M. Schatzman, *Evolution geometrique d’interfaces*, CRAS Ser. I Math. **309** (1989), 453–458.
- [9] Weinan E, Weiqing Ren, and Eric Vanden-Eijnden, *Minimum action method for the study of rare events*, Comm. Pure App. Math. **57** (accepted for 2004).
- [10] Selim Esedoglu and Jianhong Shen, *Digital inpainting based on the Mumford-Shah-Euler image model*, Euro. Jnl. of Applied Mathematics **13** (2002), pp. 353–370.
- [11] L. C. Evans, H. M. Soner, and P. E. Souganides, *Phase transitions and generalized motion by mean curvature*, CPAM **45** (1992), 1097–1123.
- [12] William G. Faris and Giovanni Jona-Lasinio, *Large fluctuations for a nonlinear heat equation with noise*, J. Phys. A: Math. Gen. **15** (1982), 3025–3055.
- [13] Hans C. Fogedby, John Hertz, and Axel Svane, *Domain wall propagation and nucleation in a metastable two-level system*, Phys. Rev. E **70** (2004), 031105.
- [14] Mark I. Freidlin and A.D. Wentzell, *Random Perturbations of Dynamical Systems*, Springer-Verlag, 2nd edition, New York, 1998.
- [15] T. Funaki, *The scaling limit for a stochastic PDE and the separation of phases*, Probab. Theory Related Fields **102** (1995), 221–288.



- [16] G. Fusco and J. K. Hale, *Slow-motion manifolds, dormant instability, and singular perturbations*, J. Dynam. Differential Equations **1** (1989), 75–94.
- [17] Morton E. Gurtin and Hiroshi Matano, *On the structure of equilibrium phase transitions within the gradient theory of fluids*, Quart. Appl. Math. **46** (1988), 301–317.
- [18] H. Hadwiger, *Gitterperiodische punktmengen und isoperimetrie*, Monatsh. Math. **76**, (1972), 410–418.
- [19] J. Hutchinson and Y. Tonegawa, *Convergence of phase interfaces in the van der Waals-Cahn-Hilliard theory*, Calc. Var. PDEs **10** (2000), 49–84.
- [20] Tom Ilmanen, *Convergence of the Allen Cahn equation to Brakke’s motion by mean curvature*, J. Differential Geom. **38** (1993), 417–461.
- [21] Robert V. Kohn, Maria G. Reznikoff, and Yoshihiro Tonegawa, *The sharp-interface limit of the Allen Cahn action in one spatial dimension*, in preparation.
- [22] Robert V. Kohn, Maria G. Reznikoff, and Eric Vanden-Eijnden, *Magnetic elements at finite temperature and large deviation theory*, to appear in JNLS.
- [23] Matthias Kurzke, *Boundary vortices in thin magnetic films*, MPI MIS Preprint 14/2004, accepted for publication in Calc. Var. PDE.
- [24] S. Luckhaus and L. Modica, *The Gibbs-Thompson relation within the gradient theory of phase transitions*, Arch. Rational Mech. Anal. **textbf107** (1989), 71–83.
- [25] Robert Marcus, *Stochastic diffusion on an unbounded domain*, Pacific J. Math. **84** (1979), 143–153.
- [26] Luciano Modica, *The gradient theory of phase transitions and the minimal interface criterion*, Arch. Rational Mech. Anal. **98** (1987), 123–142.
- [27] Luciano Modica and Stefano Mortola, *Il limite nella  $\Gamma$ -convergenza di una famiglia di funzionali ellittici*, Boll. Un. Mat. Ital. A **14** (1977), 526–529.
- [28] R. Moser, *Boundary vortices for thin ferromagnetic films*, Arch. Rat. Mech. Anal **174** (2004), 267–300.
- [29] R. Moser, *Ginzburg-Landau vortices for thin ferromagnetic films*, Appl. Math. Res. Ex. **1** (2003), 1–32.

- [30] Roger Moser, *A higher order asymptotic problem related to phase transitions*, preprint (2004).
- [31] Weiqing Ren, *Numerical methods for the study of energy landscapes and rare events*, Ph.D. thesis, New York University, 2002.
- [32] Yu. G. Reshetnyak, *Weak convergence of completely additive vector functions on a set*, Siberian Math. J. **9** (1968), 1039–1045; translated from Sibirskii Matematicheskii Zhurnal **9** (1968), 1386–1394.
- [33] Maria G. Reznikoff, *Rare Events in Finite and Infinite Dimensions*, Ph. D. thesis, New York University, 2004.
- [34] Maria G. Reznikoff and Eric Vanden-Eijnden, *Rare events on large domains: a reduction of stochastic pde dynamics*, in preparation.
- [35] Antonio Ros, *The isoperimetric problem*, Lecture Notes at the Clay Mathematics Institute Summer School, 2001.
- [36] Jacob Rubinstein, Peter Sternberg, and Joseph B. Keller, *Fast reaction, slow diffusion, and curve shortening*, SIAM J. Appl. Math. **49** (1989), 116–133.
- [37] E. Sandier and S. Serfaty, *Gamma-convergence of gradient flows and application to Ginzburg-Landau*, Comm. Pure Appl. Math. **57** (2004), 1627–1672.
- [38] Yoshihiro Tonegawa, *Phase field model with a variable chemical potential*, Proc. Roy. Soc. Edinburgh **132A** (2002), 993–1019.
- [39] S.R.S. Varadhan, *Large Deviations and Applications*, SIAM, Philadelphia, 1984.